



DESIGN STUDY AND FEM SIMULATIONS OF  
PRESSURE RESISTANT PHOTOMULTIPLIER  
ENCAPSULATIONS FOR THE LENA DETECTOR



Faculty of Physics

E 15

Lehrstuhl für  
Experimentelle  
Astroteilchenphysik

**Bachelor thesis  
of  
German Beischler**

Advisor: Prof. Dr. Lothar Oberauer  
August 8th, 2011

# Abstract

The LENA (Low Energy Neutrino Astronomy) experiment is a proposed large-scale liquid-scintillator detector, designed for the observation of low-energy neutrinos and the search for the proton decay. Neutrinos are only subject to the weak interaction and therefore have very small interaction cross-sections. The proton decay is a reaction predicted by several theoretical models beyond the Standard Model, with an expected lifetime in the order of  $10^{33}y$ . Both physics goals require a very high detector mass, posing a challenge for the detector design. With a mass of 50kt, LENA is planned with a diameter of 30m and a height of 100m. However, the resulting hydrostatic pressure on the photomultiplier tubes is one of the biggest concerns. One option to prevent the photomultiplier tubes from breaking is the use of encapsulations. Therefore, a systematic study on encapsulation forms was carried out in this thesis, based on the CAD program SolidWorks using the "Finite Element Method". Conical and spherical encapsulation forms were modeled for 3 Hamamatsu photomultiplier tubes (R5912, R7081 and R6594), with the R6594 being also modeled with an elliptical and cylindrical encapsulation. Based on a pressure of 12 bar a static study on pressure resistance was performed, eventuating in prototype encapsulations which meet the requirements of LENA. The last part of this thesis covers briefly the arrangement and installation of the photomultiplier tubes on the inner surface of the detector.

# **Table of contents**

1. Introduction.....	3
2. The LENA project .....	5
2.1 Physical goals.....	5
2.2 Detector design .....	6
2.3 Photomultipliers.....	7
3. Pressure-resistant Photomultiplier encapsulations .....	10
3.1 Encapsulation designs .....	10
3.2 Simulation with SolidWorks .....	12
3.3 Encapsulations for the Hamamatsu R5912 PMT.....	17
3.3.1 Conical encapsulation.....	18
3.3.2 Spherical encapsulation.....	20
3.4 Encapsulations for the Hamamatsu R7081 PMT.....	22
3.4.1 Conical encapsulation.....	23
3.4.2 Spherical encapsulation.....	25
3.5 Encapsulations for the Hamamatsu R6594 PMT.....	27
3.5.1 Conical encapsulation.....	28
3.5.2 Spherical encapsulation.....	30
3.5.3 Elliptical encapsulation.....	32
3.5.4 Cylindrical encapsulation.....	34
4. PMT arrangement in the inner detector .....	37
5. Summary and outlook .....	39

# 1. Introduction

“Of all the things that make the universe, the commonest and weirdest are neutrinos. Able to travel through the earth like a bullet through a bank of fog, they are so shy that half a century after their discovery we still know less about them than all the other varieties of matter that have ever been seen.” [1] Frank Close (Professor of Physics, University of Oxford).

Today we know that there are three types of neutrinos with masses under  $45.6 \frac{GeV}{c^2}$ , half the mass of the  $Z^0$  boson, over whose decay the number of lepton families can be determined: The electron- ( $\nu_e$ ), muon- ( $\nu_\mu$ ), and tau-neutrino ( $\nu_\tau$ ). The index in the symbols denotes the neutrino flavor. Figure 1 gives an overview of the hierarchy of leptons [2]. For each of these particles a corresponding antiparticle exists. In the Standard Model neutrinos are assumed to be massless, but the occurrence of neutrino oscillations prove that at least two neutrinos have masses, as for oscillations to take place the square of the mass difference has to be unequal to zero. These quantum mechanical oscillations can change the flavor of a neutrino

Leptons spin = 1/2		
Flavor	Mass GeV/c <sup>2</sup>	Electric charge
$\nu_e$ electron neutrino	$<1 \times 10^{-8}$	0
e electron	0.000511	-1
$\nu_\mu$ muon neutrino	$<0.0002$	0
$\mu$ muon	0.106	-1
$\nu_\tau$ tau neutrino	$<0.02$	0
$\tau$ tau	1.7771	-1

Figure 1: Properties of the leptons. [2]

over time due to the tilt of the mass eigenstates compared to the flavour eigenstates.

Natural sources of neutrinos encompass the fusion processes in stars as for example the Sun, the decay of radioactive isotopes in the Earth, Supernovae (which indeed confer about 99% of the released energy to neutrinos), reactions of cosmic radiation with nuclei in the earth’s atmosphere, as well as beta decays of the fission products in nuclear reactors.

As neutrinos are neutral particle, they are not affected by the electromagnetic forces. Because they are leptons the only force remaining to convey a collision with other particles is the weak interaction. This explains the extremely small cross-section for interactions with matter. So, very large detectors are needed to measure the fluxes of natural or artificial neutrino sources.

One such experiment is the planned LENA detector (Low Energy Neutrino Astronomy), which will be the subject of this thesis.

In the following in chapter 1, the goals of the physics program of LENA will be discussed shortly. Furthermore, before explaining the photosensors used in the detector, an overview over the detector design is given. As it turns out, the pressure tolerance of currently available photomultiplier tubes (PMT) series is too low to be able to use them in the detector due to the large hydrostatic pressure. The solution of this problem is the use of pressure-withstanding encapsulations housing the PMTs. In this thesis possible designs for these encapsulations are discussed and their stability is studied using SolidWorks and a

Finite Elements Method (FEM) approach. Discussing this necessity of using encapsulations is done in chapter 2. Furthermore, the method used to test the pressure resistance of possible designs is explained. After that follows the discussion of the results for all designed encapsulations in detail. Chapter 3 addresses shortly possible layouts of PMT arrangement on the inner detector. Finally, the results are summarized and possible improvements and further studies are discussed in chapter 4.

## 2. The LENA project

LENA is a proposed next generation neutrino observatory, based on 50kt of liquid-scintillator. The detector layout will be covered in chapter 2.2. The results expected for this detector are promising given the success of the KAMLAND and BOREXINO experiments, as its large volume offers the sensitivity needed to detect very low neutrino fluxes with sufficient statistics.

### 2.1 Physical goals

The physics program of LENA can be split up in two sections: Low energy physics and physics with respective energies in the orders of GeV.

Neutrinos originating from nuclear reactions as in Supernovae, the Sun, the Earth or power plants have energies in the order of MeV. The investigation of these neutrinos will be a key focus of LENA.

A Supernova occurring in the Milky Way would produce an extremely high neutrino flux, whose time dependence could be detected with high statistics and flavor sensitivity by LENA. These neutrinos are released by the conversion of protons to neutrons when the dying star collapses [3]. For Supernovae in the center of our galaxy 15,000 neutrino events are expected. In addition to obtaining new information about the processes occurring in a Supernova, LENA might be able to measure the angle  $\vartheta_{13}$  of neutrino oscillations more precisely and determine the neutrino mass hierarchy [4].

LENA will also be sensitive to diffuse Supernovae background neutrinos with an expected rate of about ten events per year [3]. By this, LENA could allow to measure the average Supernova neutrino spectrum.

The discrepancy between the expected and the measured rate of neutrinos originating from fusion reactions in the Sun was the first indication for the occurrence of neutrino oscillations. In LENA it is planned to measure the time dependence of the neutrino flux from different processes and further analyze the energy dependence of neutrino oscillations in the Sun. Furthermore, one could learn more about the elemental composition in the core of the Sun [4].

In addition LENA offers the possibility to improve the knowledge of the Earth. In the beta decays of Potassium, Uranium and Thorium, which are present in trace amounts in the Earth's crust and mantle, electron antineutrinos with energies in the range of several MeV are produced. These neutrinos can be detected via inverse beta decay. LENA could allow determining the abundance of Uranium and Thorium of the Earth's crust and mantle [4]. Also, a crucial subject is the heat flow in the Earth's interior, produced by radioactive

isotopes. Currently it is unknown to which degree the total surface heat flow originates from radioactive decays [3].

LENA would also be sensitive to neutrinos originating from the annihilation or decay of light dark matter particles. LENA could thereby to set general limits on the dark matter annihilation cross-sections and on the dark matter lifetime [5].

In the GeV energy range, LENA may obtain scientific findings regarding the postulated proton decay. In most SUSY, SU(5) models the predicted decay mode is  $p = K^+ + \bar{\nu}$ . In Cherenkov detectors the produced kaon can't be detected, because its kinetic energy is below the Cherenkov-threshold. In LENA the kaon and its decay products are detectable, which allows to substantially improve the detection probability of this proton decay mode compared to previous experiments. If no proton decay signal is detected during ten years of measurement, LENA would see a lower boundary of the partial proton lifetime due to this decay mode of  $4 \cdot 10^{34}$  years. This is one order of magnitude higher than the present limit set by the Super-Kamiokande detector [4].

Finally, LENA could be used as the far detector of a long-baseline neutrino beam experiment. The detector should be placed in the first oscillation maximum. Typical distances from the beam source range between several 100 to several 1000 kilometers. With LENA the present upper limit for the value of the mixing-angle  $\vartheta_{13}$  of neutrino oscillations could be lowered significantly, and the CP-violating phase  $\delta$  and the neutrino mass hierarchy could be determined [3]. Furthermore, through measurement of atmospheric neutrinos  $\vartheta_{23}$  could be measured more precisely.

## 2.2 Detector design

The detector is planned to be placed about 1400 meters beneath the Earth's surface as a natural shielding against muons produced by cosmic rays [4]. Because of the strong forces resulting from such depths, the detector will be installed in an oval-shaped cavern. Figure 2 shows the planned detector layout [6]. Inside the cavern a cylindrical steel tank with a height of 100m and a diameter of 30m is placed. The volume between the steel tank and the cavern wall will be filled with ultrapure water, which will act on the one hand as an additional shielding against gamma rays produced in radioactive decays and fast neutrons from spallation processes of atmospheric muons on nuclei in the surrounding rock, and on the other hand as a Cherenkov detector. To this end about 3000 photomultipliers will be mounted on the exterior wall of the steel tank [6]. Inside the steel tank a cylindrical nylon vessel will be located. The space between both cylinders will be filled with an organic liquid to further shield the actual sensitive volume, the liquid scintillator contained in the inner cylinder, from radioactivity and fast neutrons. Physical events are detected via the scintillation light produced by excitations of scintillator molecules, which are excited through collisions of charged particles moving through the detector. The detection of this scintillation

### Detector layout:

- Liquid scintillator ca. 50kt LAB.
- Inner vessel (Nylon). Radius 13m.
- Buffer (inactive liquid scint.)  $\Delta r = 2\text{m}$
- Cylindrical steel tank, 45k PMTs (8") with Winston Cones  
 $r=15\text{ m}$ , height = 100m.  
Optical coverage: 30%.
- Water cherenkov muon veto 3000 PMTs,  $\Delta r > 2\text{m}$  to shield fast neutrons
- Cavern egg-shaped for increased stability
- Rock overburden: 4000mwe

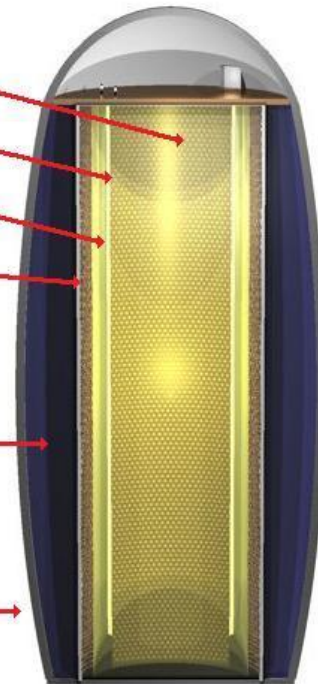


Figure 2: The detector layout [6]

light is done with photosensors mounted on the surface of the steel tank. At the moment, it is planned to use 45,000 photomultipliers (PMT) with 8" diameter, high quantum efficiency photocathodes and light concentrators attached to their front as photosensors. But also PMTs with smaller and larger diameters as well as Silicon photomultipliers have been discussed. Winston cones affixed on the encapsulations of the photomultiplier tubes enlarge the photosensitive surface of each photomultiplier. The targeted optical coverage of the steel tank's inner wall surface amounts to 30% [6].

## 2.3 Photomultipliers

Photomultiplier tubes (PMTs) are used to detect photons by converting them into an electric signal. In Figure 3 the layout of a photomultiplier tube is depicted schematically [7]. A PMT consists of two parts contained in a glass vacuum tube. First, the so-called photocathode, a thin layer of metal with a very low work function, which is evaporated on an input window on the front. A photon entering the photomultiplier tube through the input window can free electrons in the photocathode via photoelectrical effect with a certain probability. These photoelectrons are then accelerated by a voltage and focused by focusing electrodes onto an electron multiplier. By traversing the acceleration voltage the photoelectron knocks out

several secondary  $e^-$  from a so-called dynode. This process is repeated several times until a measurable signal is produced and read out at the anode [7].

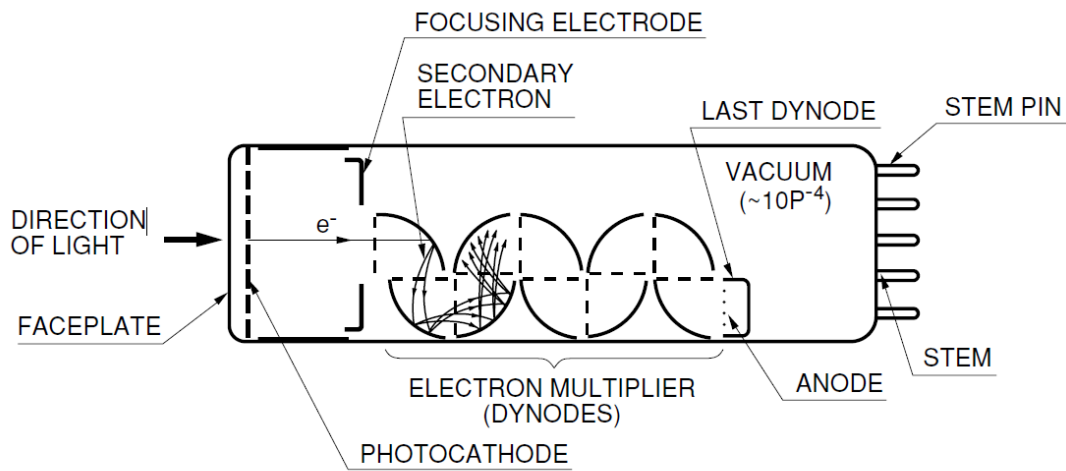


Figure 3: Schematic layout of a photomultiplier tube [7]

The photomultiplier tubes to be used for LENA have to meet various requirements to guarantee the success of LENA.

The planned value of the photo detection efficiency (PDE) is at least 20% at 420nm. The PDE is determined by the quantum efficiency of the photocathode, the collection efficiency of the photoelectrons at the anode and backscattering losses. Ideally the PDE wavelength dependence is maximized at the effective scintillator emission spectrum. That means the sensitivity of the photosensors has to be adjusted to the spectrum of the scintillation light. The transit time spread, the timing uncertainty of the detected pulses should be low. A value of less than 3ns is FWHM (Full Width Half Maximum) is targeted for LENA. Dark noise, pulses occurring without incident photons due to radioactivity, should be low as possible.

Another important source of noise are afterpulses. Afterpulses are additional pulses occurring after a primary pulse. Therefore, they might impede the detection of fast double peak structures, like proton decay events [7].

Three candidate PMT series most probably meeting these requirements are the Hamamatsu R6594 (5" diameter), R5912 (8" diameter) and R7081 (10" diameter), which were studied in this theses. Another currently considered is Electron Tubes Enterprises, as the relevant series have also diameters of 5" and 8".

The necessity to employ pressure resistant photomultiplier encapsulations arises from the huge proportions of the LENA detector. The 100m head of scintillator liquid exerts a high pressure of 10 – 11 bar, depending on the composition of the scintillator, on the lower photomultiplier tubes. Standard photomultiplier tubes only resist a pressure of 7 – 8 bar. There are two opportunities to solve this problem. The first one is using custom-build PMTs with thicker glass. The problem with this is, no experiences were made with such tubes till

now, so it is not sure that the pressure withstanding is given by the modified PMTs. In addition, the attributes of the PMTs may change. Another big disadvantage is, that more material is used, causing more radioactivity. So far, the second opportunity is more favorable: research projects like BOREXINO, ANTARES or ICECUBE use encapsulations, housing the PMTs, to make sure no PMT gets damaged. In order to absorb the forces resting on the tubes, the encapsulation must be sturdy enough and may not deform over a certain point to ensure the safety of the PMTs. In this bachelor thesis potential designs of encapsulations for candidate PMT series are simulated with an applied pressure of 12 bar to determine the necessary thickness of the used materials. To underline the importance of pressure encapsulations, the Japanese Super-Kamiokande detector can be given as an example. This neutrino detector consists of a stainless steel tank of 39m diameter and 42m height. It is filled with 50,000 ton of ultrapure water, which results in an ambient pressure of about 4.2 bar on the bottom of the tank. The tanks walls are covered with 11,146 20" PMTs. Figure 4 shows the Super Kamikande detector during the filling stage [8].

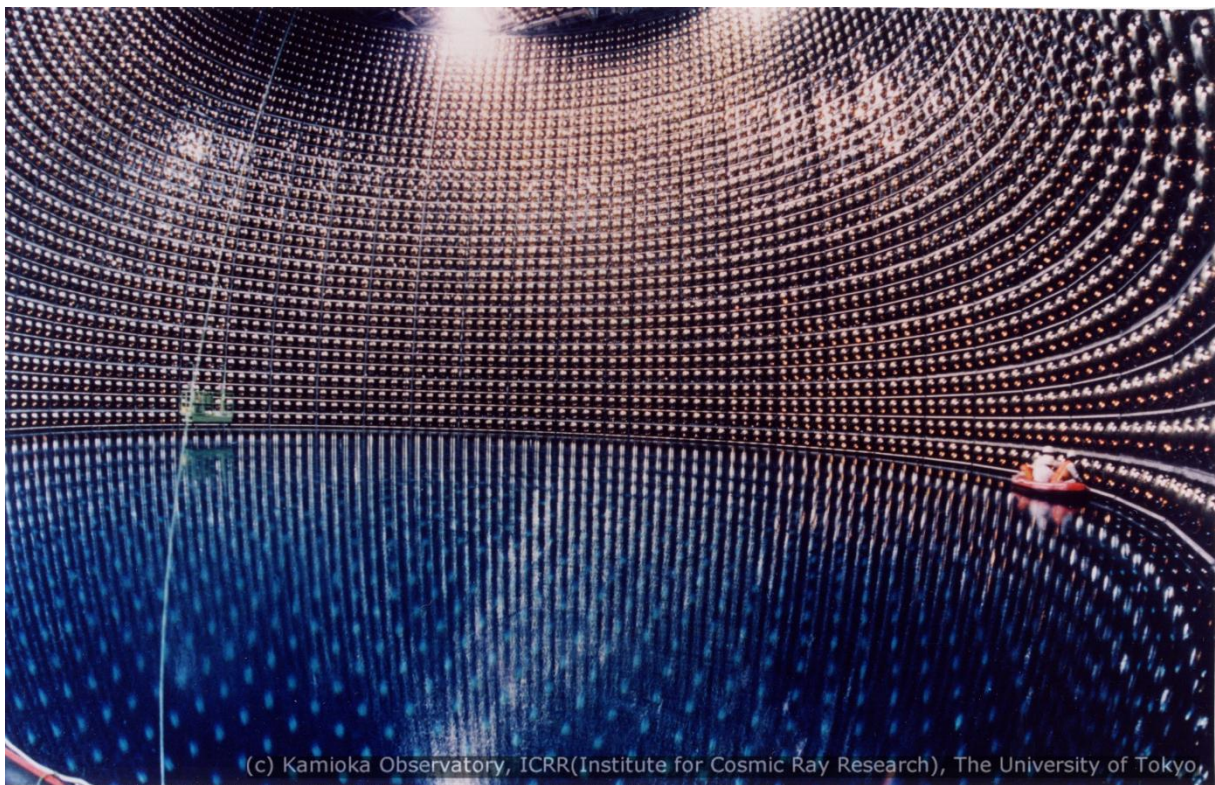


*Figure 4: The Super-Kamiokande detector, during the filling [8].*

When Super-Kamiokande began data taking on April 1st, 1996, no pressure resistant encapsulations for these photomultipliers were used. From July to September 2001 the water was pumped out to allow maintenance work as replacing defective PMTs. On November 12th the work in the tank was finished and the purified water was refilled to a level of 31.7 meters, which is about three quarters of the detectors height. In this setup 6,665 photomultipliers imploded in a chain reaction, caused by the shock wave of a broken PMT [8]. When the detector was restored subsequently pressure resistant encapsulations were installed, to prevent such an event in the future.

### 3. Pressure-resistant Photomultiplier encapsulations

The accident in the Super-Kamiokande detector shows that pressure resistant photomultiplier encapsulations are necessary to build detectors with large dimensions. Therefore, in this bachelor thesis different encapsulation forms with varying thicknesses of the materials used were simulated under pressure. The results of these tests will be used subsequently to build prototypes, which then will be tested under real conditions in a pressurized tank.

#### 3.1 Encapsulation designs

The encapsulation designs, which were simulated in this bachelor thesis, consist, as previously employed for other detectors, like BOREXINO or ANTARES, of a metallic lower part and a transparent cap made from acrylic glass. The metallic part encloses the base, where the photomultiplier will be plugged in, which contains the voltage divider and also the power connection. This lower part has to be leak-proof for the buffer liquid, respective water for the outer detector. To ensure that, it is planned to fill up the base with Polyurethane, which was even used in the BOREXINO and DOUBLE CHOOZ encapsulations.

The metallic part of the encapsulation will cover the lower part of the photomultiplier. The upper part of the photomultiplier's glass envelope will be protected by a spherical segment made from an acrylic glass completing the encapsulation at the top. To improve stability a hemispherical form was chosen for the glass.

The simulation was carried through using 1,4404 stainless steel (X2CrNiMo17-12-2) and high impact resistant acrylic glass as materials. The first step to do any simulations was to construct the encapsulations with SolidWorks.

The layout described above was already used for other detectors. In the case of BOREXINO a metallic conical encapsulation with a thin acrylic foil in form of a spherical segment was chosen for the outer detector, as the hydrostatic pressure was only about 2 bar and no pressure absorption was needed. The lower part of the encapsulation is metallic and divided into two parts. A metallic cylinder containing the electronics is connected to the upper conical part. Dividing the encapsulation's metallic part makes it much easier to insert the base and the electronics into the encapsulation. If it would be constructed as one part, this might cause complications as the inner radius of the cylindrical part was adjusted to the dimensions of the base. In the models simulated in the bachelor theses this radius was only 35mm. The disadvantage of a two parted metallic encapsulation is the introduction of another edge where the scintillation liquid might leak into the encapsulation. Due to the time limit only the two-part metallic encapsulation could be simulated. Another difference between the encapsulations used for BOREXINO and the simulated ones is the form of the

acrylic glass, which is now not only a spherical segment but a hemisphere. The radius of this hemisphere is chosen in a way that a sufficient distance from PMT surface to the inner radius of the hemisphere is kept as to provide a best possible fit of the inner perimeter of the hemisphere to the form of the PMT. The distance is introduced as a precaution to prevent breaking of the PMT in case the acrylic encapsulation might get dent by the pressure. This deformation will be discussed shortly in the conclusions.

The form of the cone-shaped encapsulation was adjusted to match the form of the photomultiplier tube. Here one consideration was to minimize the surface area of the conical segment as a function of height of the conic section  $h_c$ . The resulting height  $h_{c,opt.}$  depends on the larger radius R and the smaller radius r and is given by:

$$h_{c,opt.} = \frac{4 \cdot r^2 \cdot (R - r)}{(R + r) - 4 \cdot r^2} \quad (1)$$

The results for  $h_{c,opt.}$  are shown in table 1:

PMT	Radius R [mm]	Radius r [mm]	$h_{c,opt.}$ [mm]	$h_{conical\ part}$ [mm]	Lateral surface [mm <sup>2</sup> ]
<b>R5912 (8")</b>	120	55	52.50	146	78,247
<b>R6594 (5")</b>	82	55	36.37	169	65,329
<b>R7081 (10")</b>	147	55	59.73	141	97,694

*Table 1: The optimized outer lateral surface of the conical encapsulation parts and  $h_{c,opt.}$  for each PMT*

By lateral surface the outer surface of the conical part of the encapsulation is meant, which was minimized.  $h_{conical\ part}$  is the height of the conical encapsulation part.

Possibly the weight and so the volume would be minimized for other values of  $h_c$ , as the encapsulations stability might depend on the height of the conical section and so for different  $h_c$  the thinnest possible wall thicknesses might change.

The other encapsulations, which were simulated, were composed of the spherical encapsulations and for the photomultiplier R6594 tube in addition an elliptical and a cylindrical encapsulation, had only one metal part instead of two. The spherical encapsulations were simulated for each photomultiplier series. Spherical pressure encapsulations for PMTs were already used in previous research projects in neutrino physics e.g. ANTARES, NEMO, NESTOR or ICECUBE. The spherical design was considered because of the natural stability of this form. The advantage of such an edgeless form is, that the areas where wall thicknesses of the encapsulations changes get reduced. At these areas arise bending strains and shear stresses. So a spherical design might allow saving material compared to conical encapsulations. Additional, material introduces radioactivity into the detector, for which reason, both surface and mass of the encapsulations should be minimized. The spherical design consists of two parts: A metal hemisphere and a hemisphere made from acrylic glass. The diameter of the whole sphere is adjusted to the total length of

the PMT and its base. Especially for the Hamamatsu R7081 due to its form the spherical encapsulation would make sense. The R6594 PMT by contrast has a very oblong form, so for this photomultiplier tube rather an also oblong encapsulation would be useful. For this reason for this photomultiplier tube in addition a cylindrical and an elliptical encapsulation were designed and tested.

## 3.2 Simulation with SolidWorks

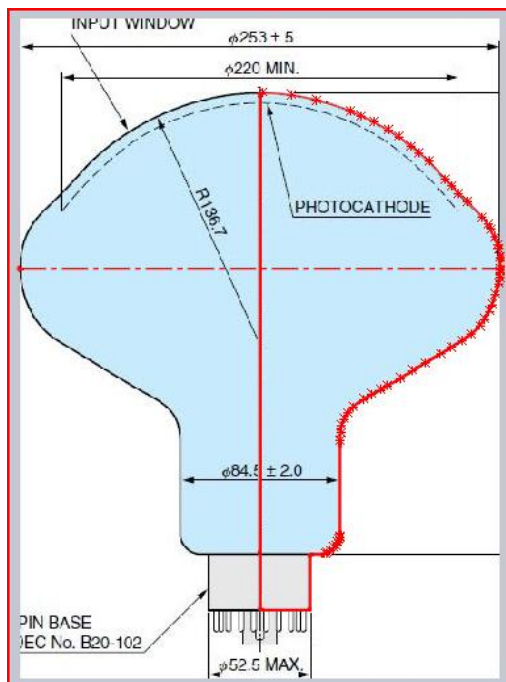


Figure 5: Photomultiplier profile with outline [10]

In order to be able to design an encapsulation requires first a model of the respective photomultiplier tube. For this reason, the engineering drawings in the original PMT data sheets from the Hamamatsu product catalogue were imported into SolidWorks. The boundary of the PMT form in the data sheet was outlined, as depicted in Figure 5 for the R7081 [10]. This outline was rotated by 360° to obtain the complete PMT form. The model was sized to match the measurements in the engineering drawings. The scaling of height and width fitted very well, with a difference of only at most 5mm, which had to be corrected. The encapsulations were fitted to these replications. To construct an encapsulation, again first its outline was defined, which then was rotated by 360° to obtain a closed surface. After that the material composition was set. SolidWorks

contains a large list with different materials. The decision to use 1,4404 stainless steel and high impact resistant acrylic glass was taken in cooperation with Mr. Hess, the senior mechanic of the chairs workshop, who is the SolidWorks expert of the chair.

The metallic segment and the acrylic glass of the encapsulation models are connected through a flange with a thickness of 6mm and a width of 30mm. In the metallic flange a groove with a width of 3.9 mm and a depth of 2.3 mm will be engraved, in which an O-ring seal will be placed. The measurements are DIN standard and were chosen after consultation with Mr. Hess. This groove was implemented in all simulated encapsulations. The tightness of the gasket has to be determined experimentally with a prototype. Also holes were integrated in the flange to screw the acrylic and the metallic section together. These screw holes will also be used to attach the light concentrators and the mounting bracket connecting adjacent encapsulations and fixing them on the inner wall. To sustain the weight of the encapsulation and the PMT another bracket in form of a small hollow cylinder was

added on the bottom of the encapsulation. In this model the connector to the high voltage cable will be placed inside this cylinder.

In chapter 4, the mounting will be discussed in more detail. Finally before starting a simulation the components of an encapsulation have to be assembled and to ensure that the parts do not overlap or have gabs in between, an analysis of the occurrence of such cases was done. Moreover SolidWorks calculates the surface, the mass and the volume of the components and the complete assembly. These resulting values for each encapsulation are given in the corresponding chapters.

To ensure that the encapsulation designs resists a pressure of 12 bar a static study was performed. Static studies in SolidWorks calculate displacements, forces, loads and stresses [9]. The simulation determines a factor of safety distribution, which is a measure of the static stability of the model. It is possible to apply a homogeny pressure to selected surfaces. SolidWorks uses the finite element method for modeling the pressure effects. This numerical method divides the modeled object by the program into small elements, which share common points called “nodes”. This procedure is called “meshing” [9]. In this way a complex problem is subdivided in more simple problems, which are solved simultaneously.

In the bachelor thesis the maximum distance of the nodes is set to 3mm with an inaccuracy of 0.15mm. Figure 6 shows the meshing of an encapsulation model with a thickness of the conic shaped part of 0.5mm and a thickness of the acrylic part of 1mm. The encapsulation is modeled for the R5912 PMT. In the later part of this section the influence of the node distance on the results of the study is discussed.

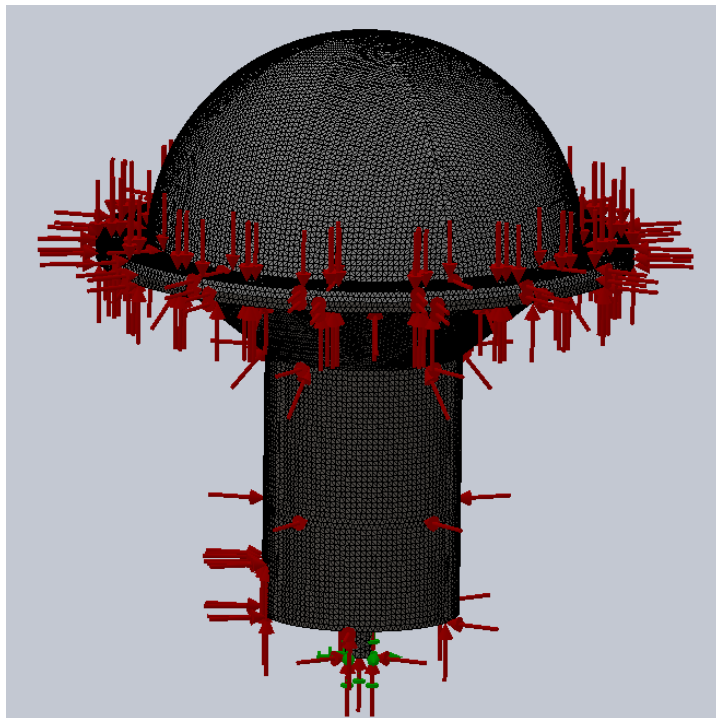
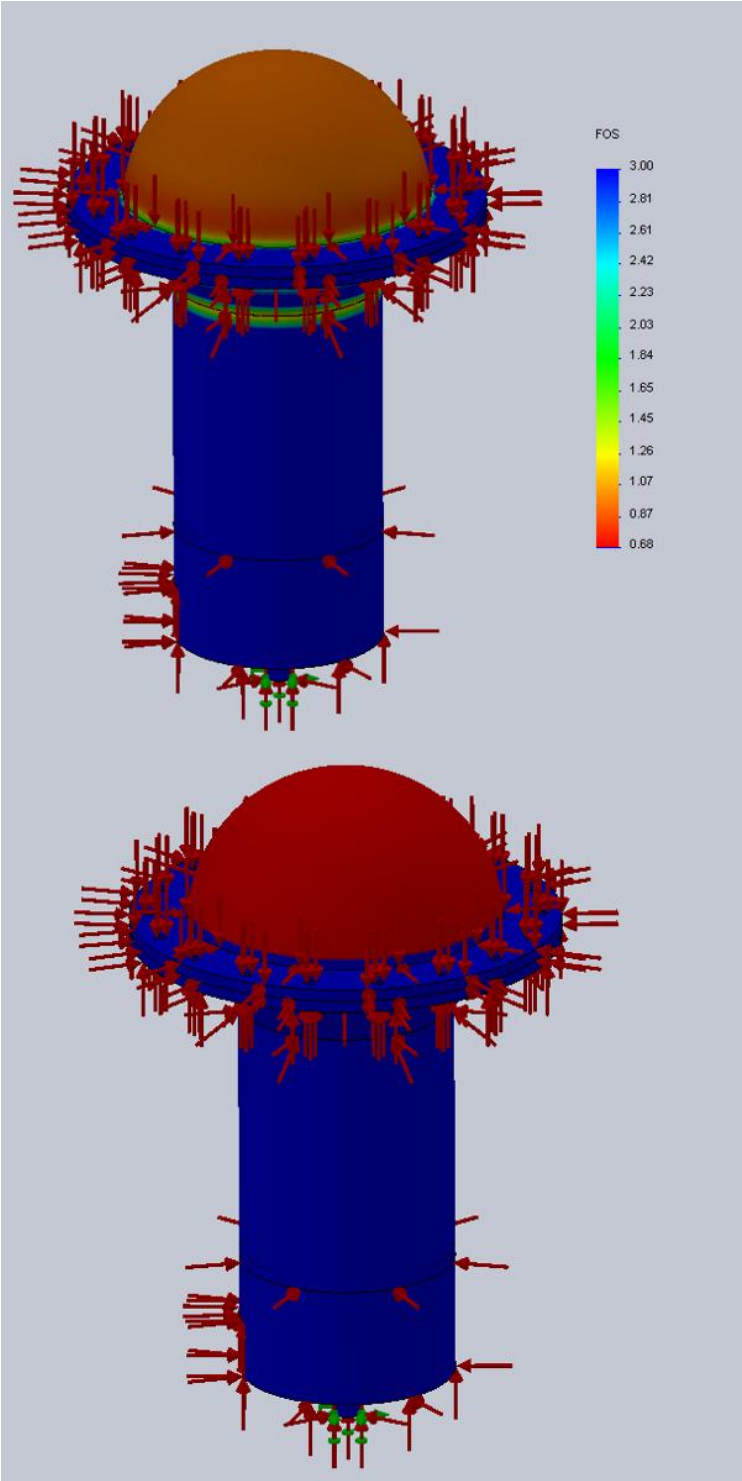


*Figure 6: Meshing of the encapsulation model (metallic thickness 0.5mm, acrylic glass thickness 1mm) for the Hamamatsu R5912 PMT with a node distance of 3mm.*

The behavior of each node under pressure is calculated and SolidWorks interpolates to every point in an element [9]. Hereby, SolidWorks takes consideration on connections of different elements. For the static studies started on our model the stress analysis finds displacements on the nodes whereby it calculates the strain and stresses. Based on that, it calculates the factor of safety distribution, as shown in Figure 7.



A factor of safety less than 1 points out material failure, which means that the encapsulation model does not withstand the pressure of 12 bar and will break. In the lower image of Figure 7, breaking parts of the model are shown red while the blue parts withstand the pressure.

*Figure 7: The factor of safety calculated on the conical mode for the R6594 PMT. The wall thickness of the metallic segment is 0,5mm and for the acrylic glass 1mm. The node distance is 3mm.*

*Above: The factor of safety. The lowest value is 0.68. All values over 3 are painted blue.*

*Down: The areas of instability, with a factor of safety below 1, are marked red.*

The factor of safety is calculated by one of four failure criteria [9]:

- *The Maximum von Mises Stress Criterion:*  
This criterion is based on the von Mises-Hencky theory. The theory implies that a material starts to yield at a point, when the “von Mises Stress” becomes equal to the stress-limit. When strain exceeds the yield point, the material does not stay elastic anymore. Finally the material will break. [9]
- *The Maximum Shear Stress Criterion:*  
The “Maximum Shear Stress Criterion” is very similar to the “von Mises Stress Criterion”. But this criterion is rather applied for ductile materials. Studies have shown that the “von Mises Stress Criterion” gives more accurate results. [9]
- *The Mohr Coulomb Stress Criterion:*  
This used for brittle materials with different tensile and compressive properties. These materials do not have a certain yield point. [9]
- *The Maximum Normal Stress Criterion:*  
Even this criterion is used for brittle materials. This criterion supposes that the materials failure limit is identical for tensions and pressure. This assumption is not right for all cases. For example decrease cracks in the material the tensile strength while their effects on pressure resistivity are rather less. [9]

If the material of the models is defined, SolidWorks uses the best fitting criterion to calculate the factor of safety.

It has to be highlighted that computational stability is an issue in the use of SolidWorks. The computer, used at the beginning of this thesis, was unable to calculate node resolutions of distances less than 3mm and gave unstable simulation results. Therefore, it was replaced by a more efficient computer. The setting of a 3mm node distance was maintained through this thesis. For a good measure, the influence of the node distance on the results of the study were tested and the results shown in Figure 8.

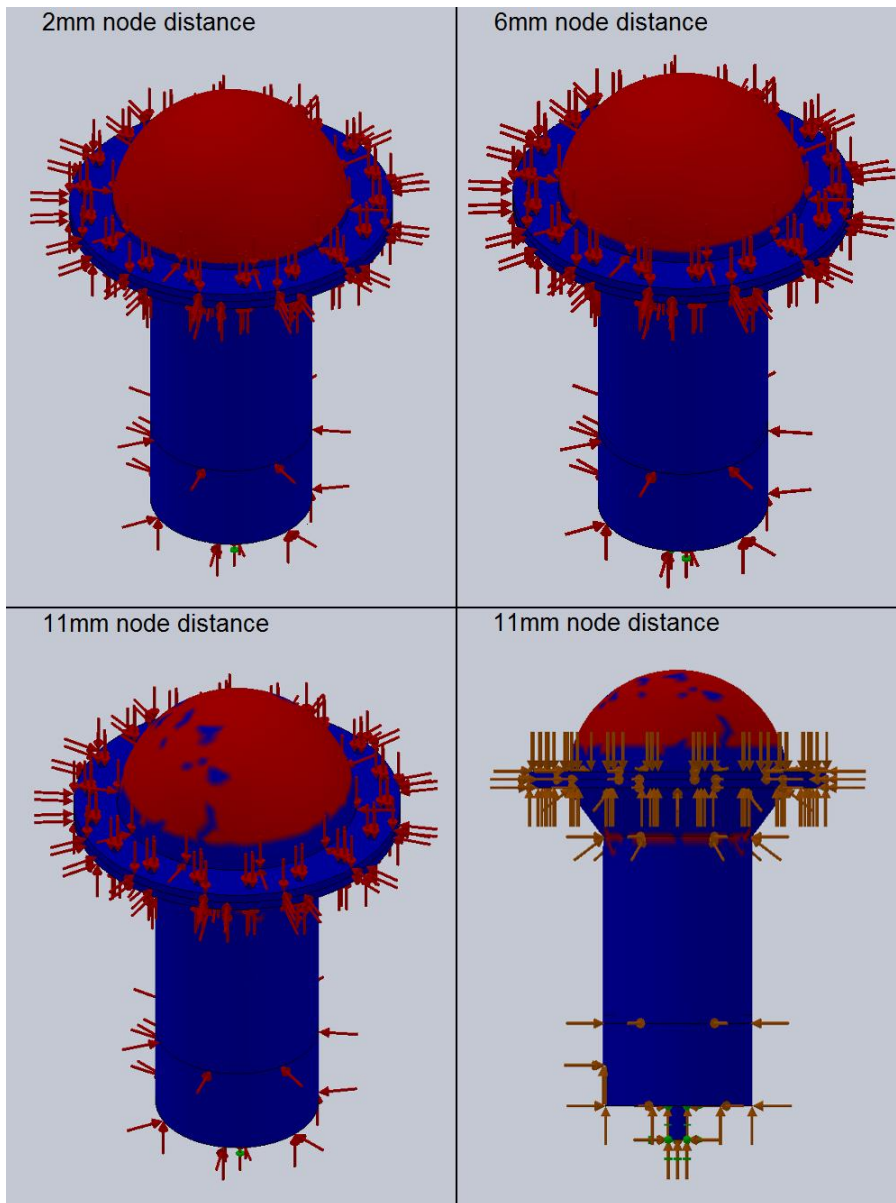


*Figure 8: The models safety for note distances of 2mm, 6mm and 11mm for the conical encapsulation of the R6594 PMT. The encapsulations thicknesses are 0.5mm stainless steel and 1mm acrylic glass. The red breaking areas, with a factor of safety below 1, changes with the node distance.*

Comparing Figure 7 and Figure 8 one can see that the difference between a node distance of 2mm and 3mm is very small on the simulation results. Meshing a smaller node distance was not possible because of processing power. Increasing the node distance indeed reduces the accuracy of the simulations.

The reproducibility of the simulations with the new computer was tested. Therefore, one simulation was done several times for the same model, giving satisfying agreement.

### 3.3 Encapsulations for the Hamamatsu R5912 PMT

The Hamamatsu R5912 is an 8" photomultiplier tube with a height of 275mm and a width of 202mm wide photomultiplier tube. In Figure 9 its profile is shown [10].

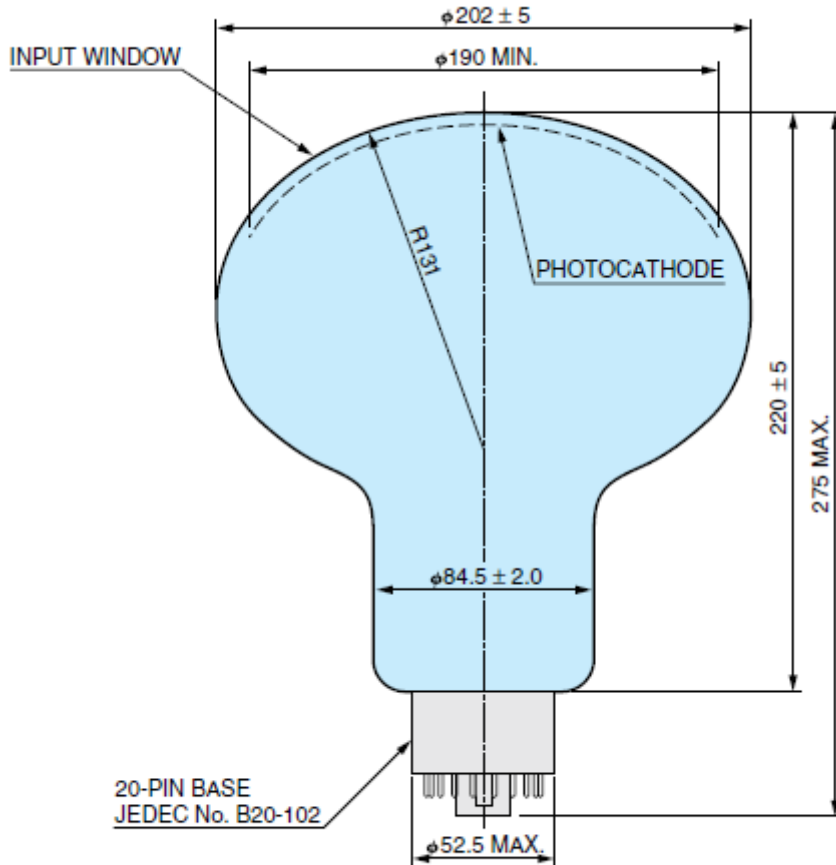


Figure 9: Profile of the Hamamatsu R5912 PMT [10]

It features a bialkali photocathode with a spectral response in the range of 300nm to 650nm and a quantum efficiency at the peak wavelength of about 25%. The typical transit time spread, the timing uncertainty of a voltage pulse amounts to 2.4ns at FWHM (Full Width Half Maximum). The anode dark current output, measured after 30 minutes in complete darkness, is for this PMT 50nA [10]. For this photomultiplier tube a conical and a spherical encapsulation were modeled and simulated.

### 3.3.1 Conical encapsulation

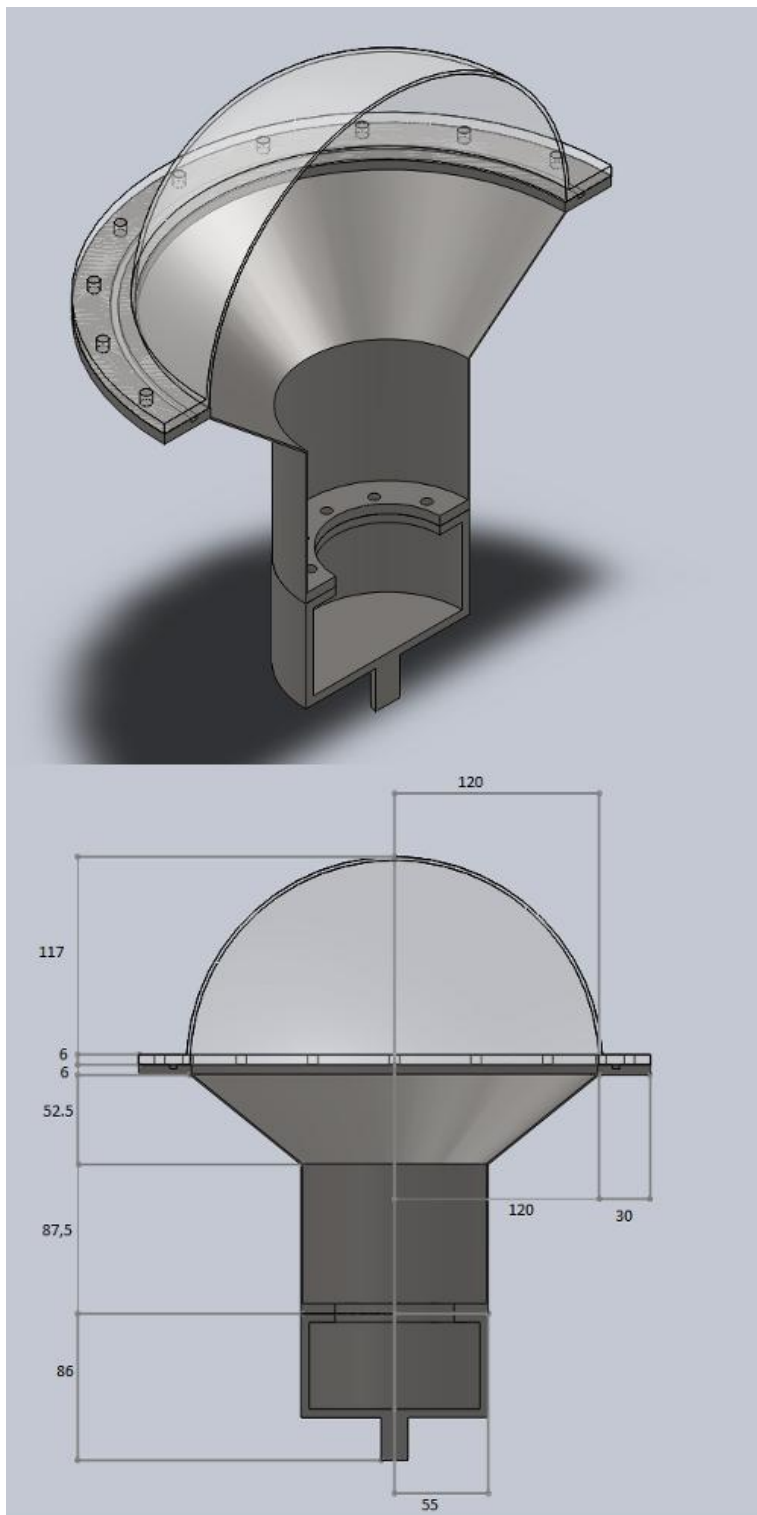


Figure 10: The conical encapsulation for the Hamamatsu R5912 PMT, which passed the stress test with the lowest thicknesses of 1mm for the metallic part and 2mm for the acrylic glass. The measurements are given in mm.

The conical encapsulation was, as stated above, inspired by the encapsulation for the BOREXINO experiment. In Figure 10 one can see the encapsulation with the lowest thicknesses, which passed the static load simulation, in profile. The total height of this encapsulation is 355mm. The upper radius is 120mm and the smaller one 55mm. This means a height  $h_{c,opt.}$  of the conic section of 52.50mm. So for the outer lateral surface an area of 782.47mm<sup>2</sup> follows. The inner radius of the acrylic glass hemisphere is 120mm.

The conical encapsulation for the R5912 with minimal thicknesses, which passes the stress simulation, consists of a metallic encapsulation of 1mm thickness plus an acrylic hemisphere of 3mm thickness. Figure 11 shows you the factor of safety for the ideal encapsulation. The overall weight of the encapsulation is 3,73kg. The materials volume is 829.25cm<sup>3</sup> and the overall surface is 5,315.85cm<sup>2</sup>, like table 2 shows.

Conical encapsulation:	Thickness metallic part:		1mm
	Thickness acrylic part:		3mm
	Volume [cm <sup>3</sup> ]	Surface [cm <sup>2</sup> ]	Weight [g]
Overall encapsulation:	829.25	5,315.85	3,733.22
Metallic part:	414.87	2,952.96	3,235.95
Acrylic part:	414.39	2,362.89	497.27

Table 2: Properties of the most lightweight stable conical encapsulation for the Hamamatsu R5912 PMT in detail.

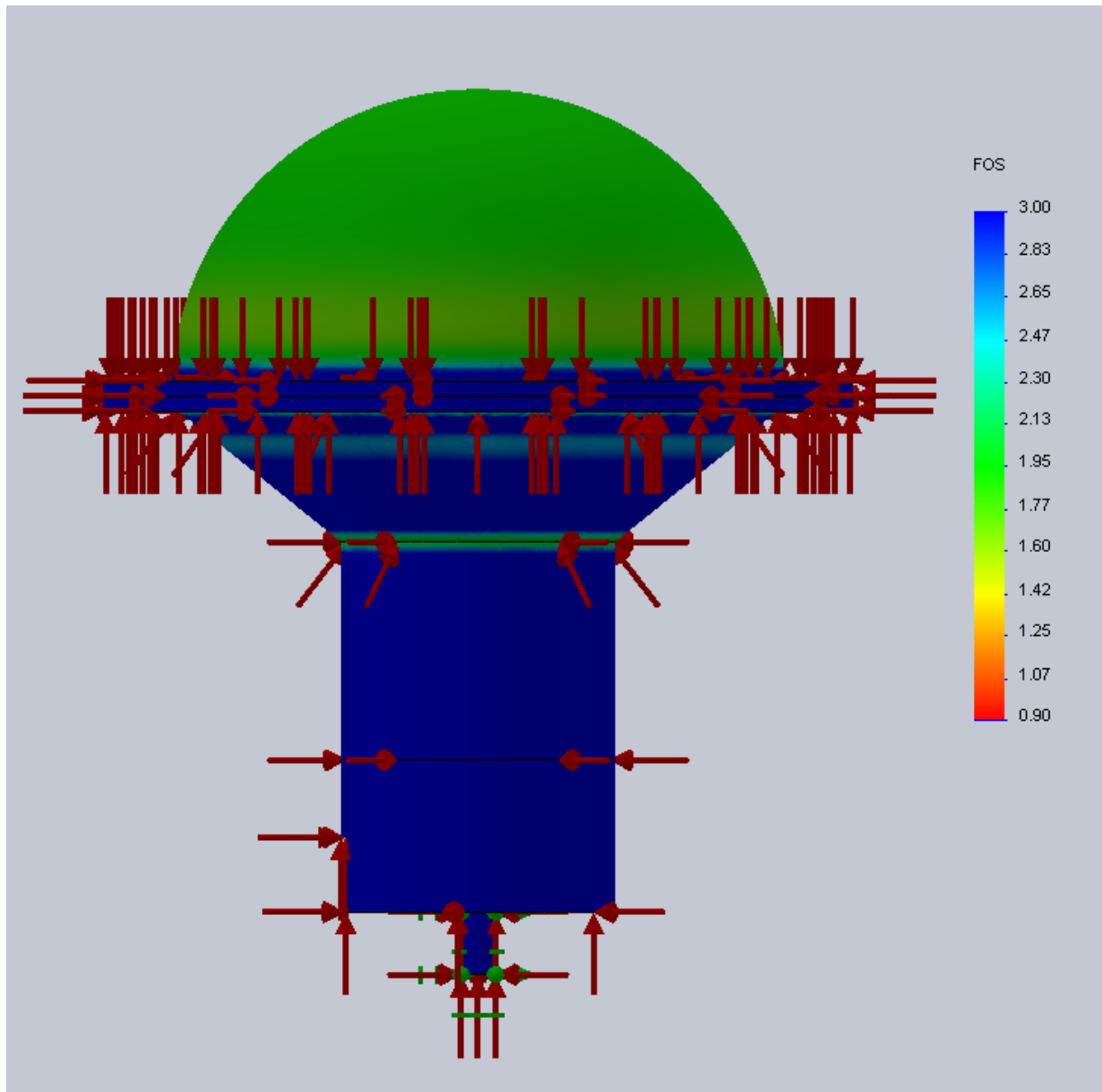
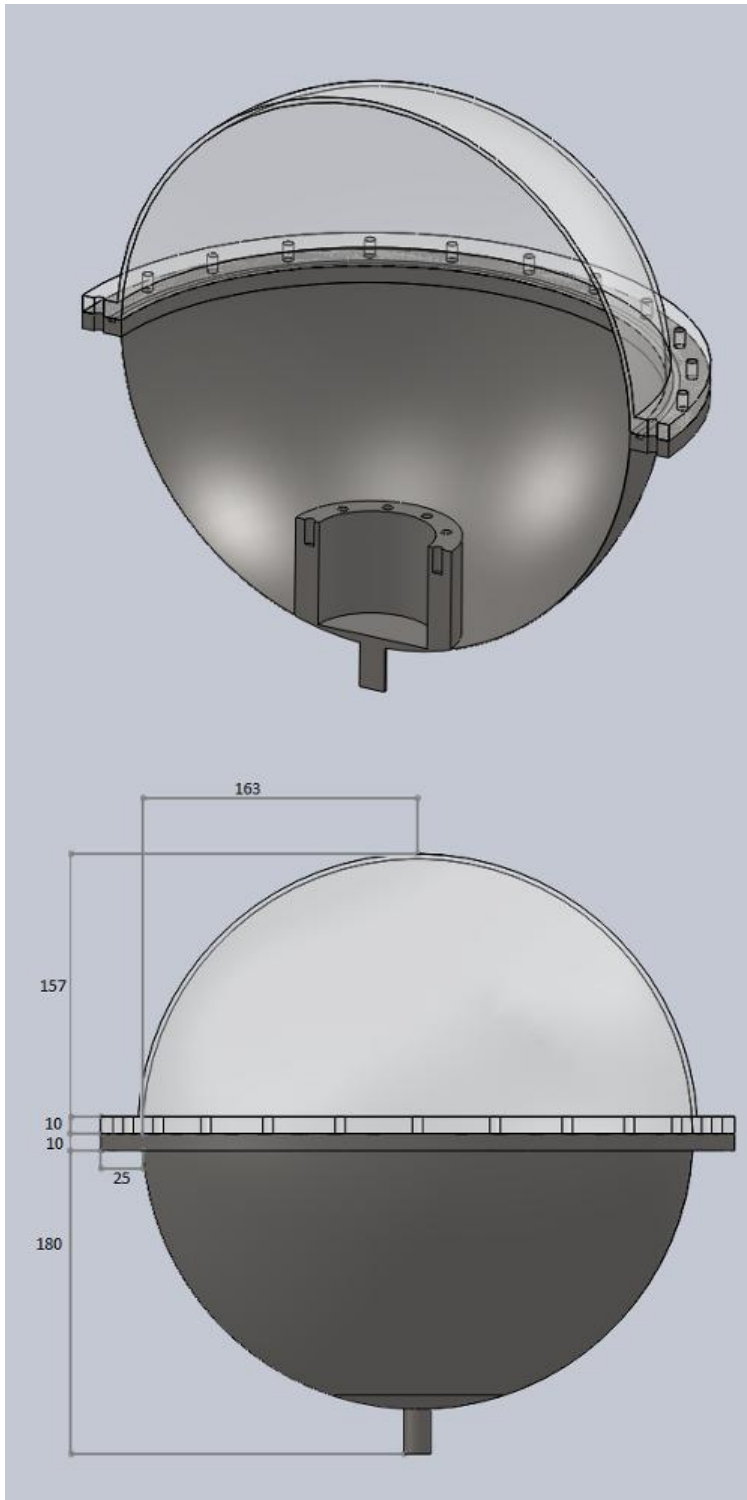


Figure 11: The factor of safety for the conical encapsulation of the R5912 PMT. The lowest value is 1.18, thus the whole PMT encapsulation withstands the requested 12 bar static pressure.

### 3.3.2 Spherical encapsulation



The spherical encapsulation for the Hamamatsu R5912 PMT was done with a diameter of 326mm. The height of the encapsulation is 357mm. Figure 12 shows the profile view of the stable encapsulation with the least material. Comparing the conical encapsulation to the spherical encapsulation with the lowest thickness is at a disadvantage. The minimal required thickness is 0.5mm for the metallic encapsulation part and 4mm for the acrylic glass. With 5.75kg the ideal spherical encapsulation is heavier and even the materials volume of  $1,509.86\text{cm}^3$  and its surface of  $8,346.03\text{cm}^2$  are bigger compared to the conical encapsulation. Table 3 contains the data of the assessed encapsulation and figure shows the factor of safety.

*Figure 12: The spherical encapsulation for the Hamamatsu R5912 PMT, which passed the stress test with the lowest thicknesses of 0.5mm for the metallic part and 4mm for the acrylic glass. The measurements are given in mm.*

Spherical encapsulation:	Thickness metallic part:		0.5mm
	Thickness acrylic part:		4mm
	Volume [cm <sup>3</sup> ]	Surface [cm <sup>2</sup> ]	Weight [g]
Overall encapsulation:	1,509.86	8,346.03	5,752.82
Metallic part:	597.12	4,366.45	4,657.53
Acrylic part:	912.74	3,979.58	1,095.29

Table 3: Properties of the most lightweight stable spherical encapsulation for the Hamamatsu R5912 PMT in detail.

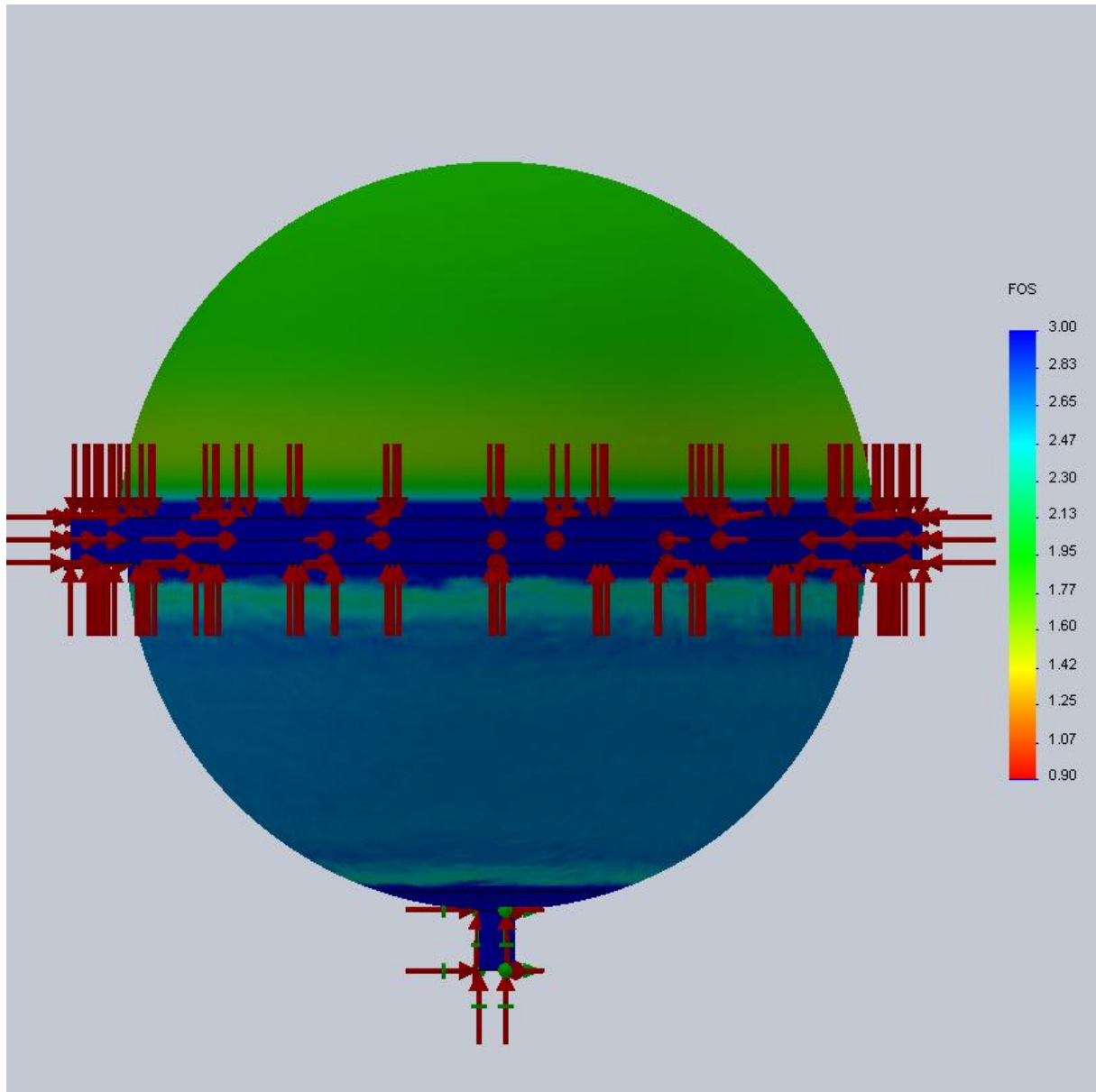


Figure 13: The factor of safety for the spherical encapsulation of the R5912 PMT. The lowest value is 1.17, thus the whole PMT encapsulation withstands the requested 12 bar static pressure.

### 3.4 Encapsulations for the Hamamatsu R7081 PMT

The Hamamatsu R7081 PMT is a 10" photomultiplier tube. Its measurements are 300mm in height and about 253mm in width. Figure 14 shows the schematics for the Hamamatsu R7081 PMT [10].

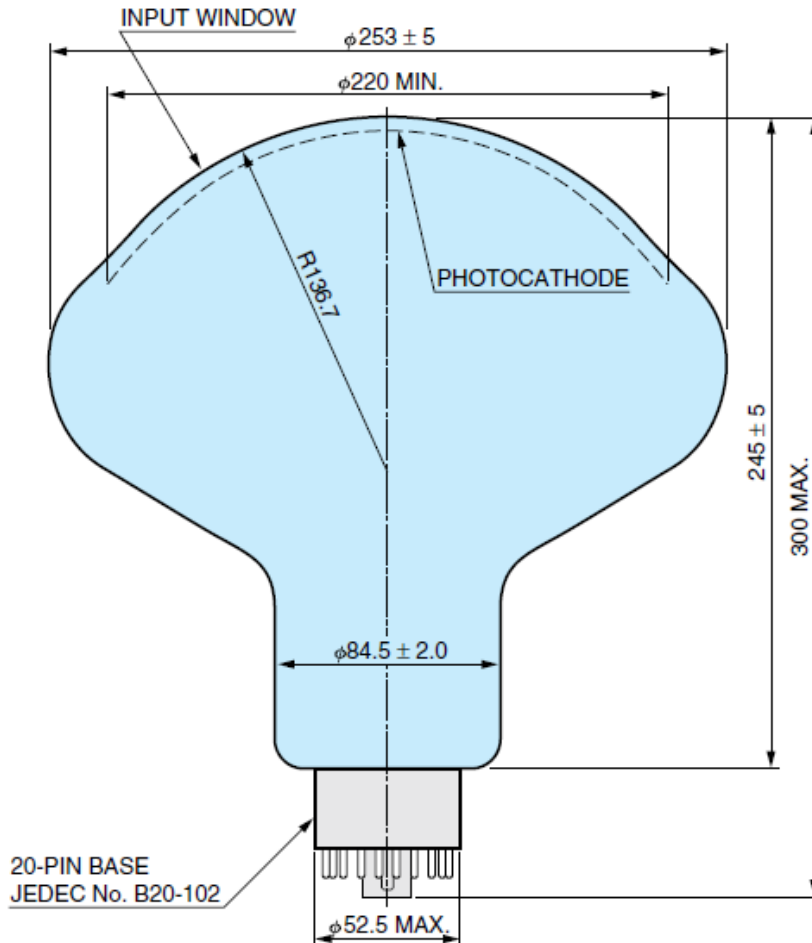


Figure 14: Profile of the Hamamatsu R7081 PMT [10]

The key features of the R7081 PMT are: The spectral response range covers 300nm to 650nm. The quantum efficiency at the peak wavelength is about 25%. The anode dark current output, measured after 30 minutes in complete darkness, is for this PMT 50nA. The transit time spread is 2.9ns at FWHM [10].

### 3.4.1 Conical encapsulation

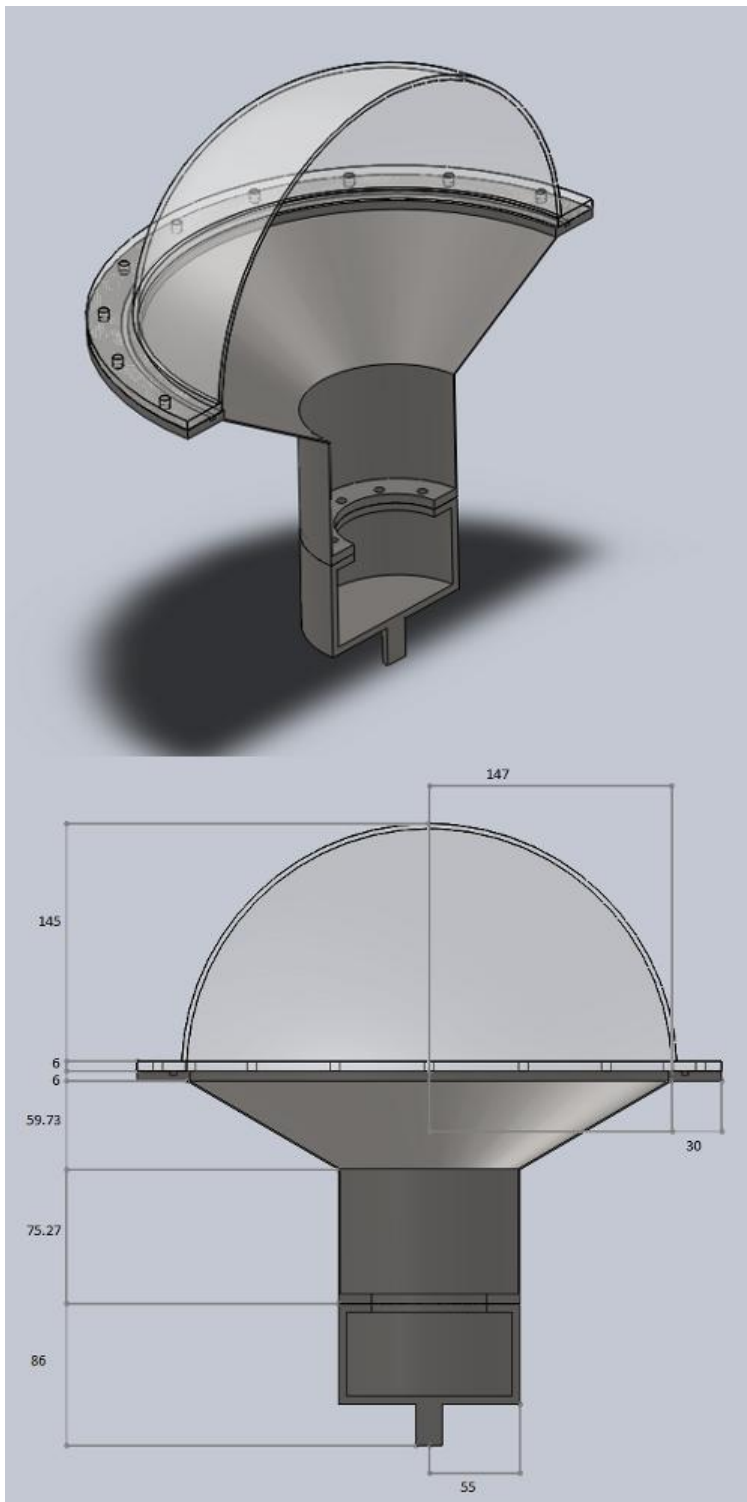


Figure 15: The conical encapsulation for the Hamamatsu R7081 PMT, which passed the stress test with the lowest thicknesses of 2mm for the metallic part and 4mm for the acrylic glass. The measurements are given in mm.

The upper diameter of the conical encapsulation for this PMT is much more expanded in comparison to the conical designs for the other two PMT types. Figure 15 shows the encapsulation passing the stress simulation. The upper radius of the metallic encapsulation is 147mm. The radius of the cylindrical end of the conical encapsulation is 55mm. So the ideal height of the conic section is 59.73mm. The all-over height of the encapsulation is 378mm. The acrylic glass is 151mm high.

The necessary thicknesses for the metallic part are 2mm and 4mm for the acrylic glass. With it the weight of the whole encapsulation is 5,24kg, the volume becomes 1,277.15cm<sup>3</sup> and the surface 6,921.98cm<sup>2</sup>. For details see Table 4. The factor of safety is shown in Figure 16.

Conical encapsulation:	Thickness metallic part:		2mm
	Thickness acrylic part:		4mm
	Volume [cm <sup>3</sup> ]	Surface [cm <sup>2</sup> ]	Weight [g]
Overall encapsulation:	1,277.15	6,921.98	5,236.68
Metallic part:	561.23	3,462.34	4,377.57
Acrylic part:	715.93	3,459.55	859.11

Table 4: Properties of the most lightweight stable conical encapsulation for the Hamamatsu R7081 PMT in detail.

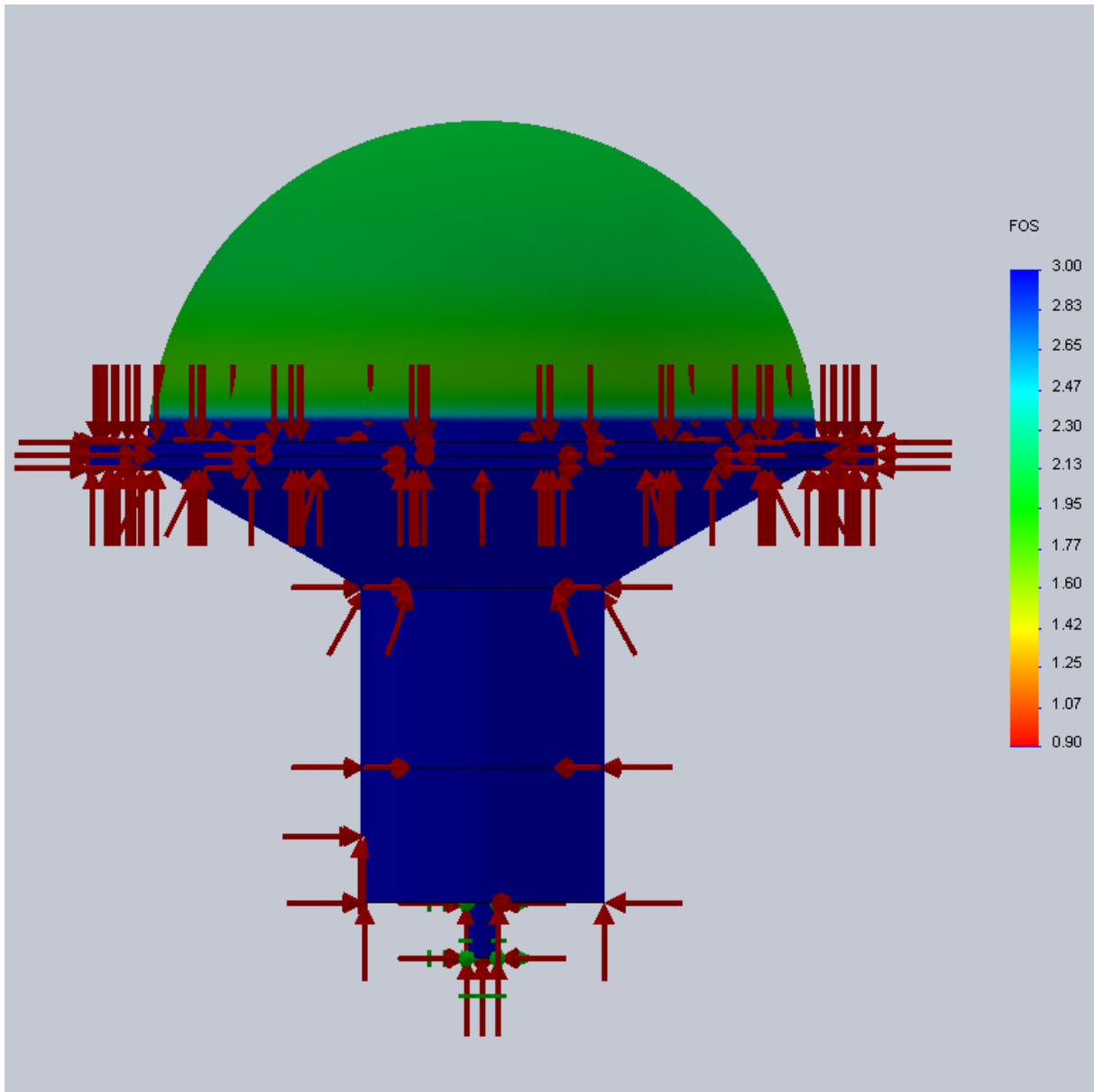
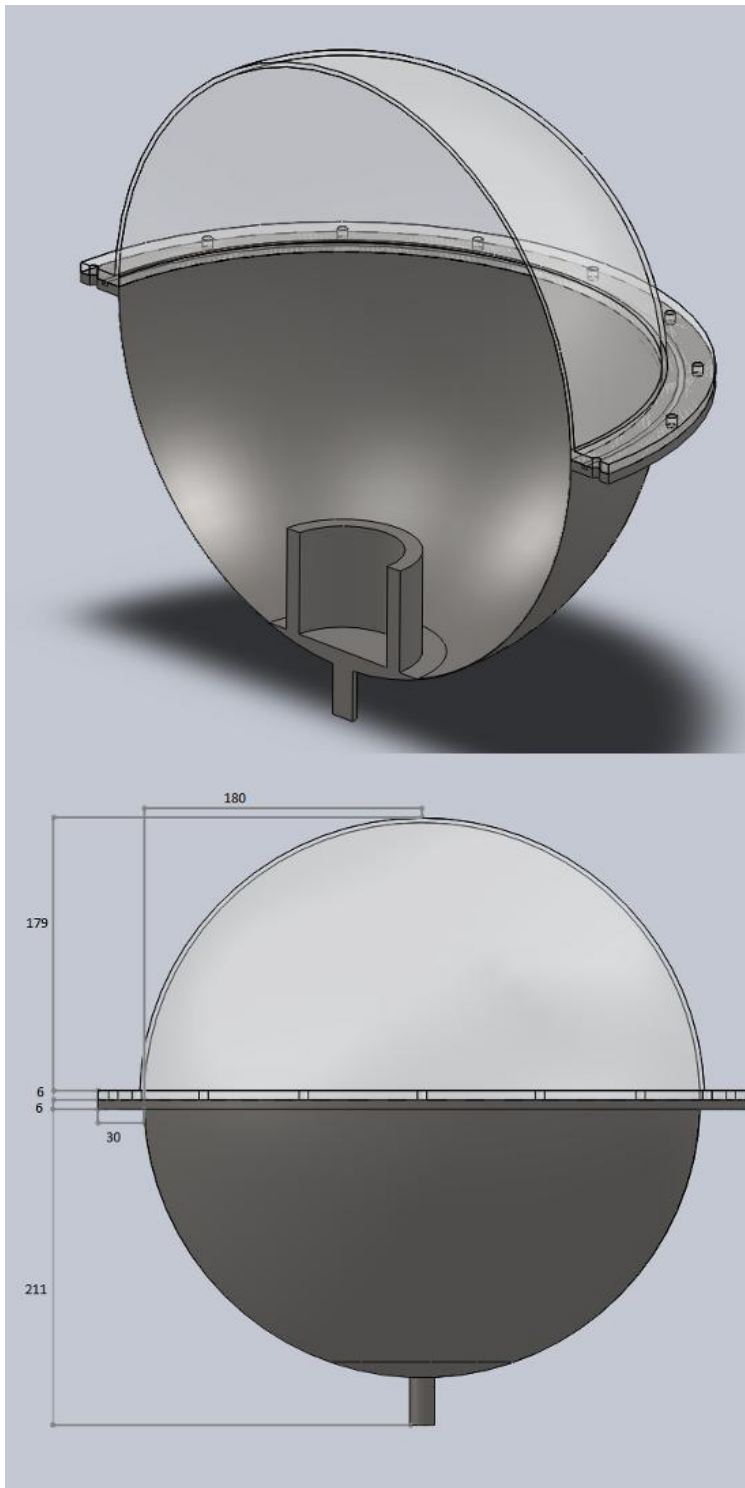


Figure 16: The factor of safety for the conical encapsulation of the R7081 PMT. The lowest value is 1.07, thus the whole PMT encapsulation withstands the requested 12 bar static pressure.

### 3.4.2 Spherical encapsulation



*Figure 17: The spherical encapsulation for the Hamamatsu R7081 PMT, which passed the stress test with the lowest thicknesses of 0.5mm for the metallic part and 5mm for the acrylic glass. The measurements are given in mm.*

The spherical encapsulation for the Hamamatsu R7081 PMT was a logical consequence, because of the photomultiplier tubes wide form. For this form a radius of 180mm was chosen. The profile view of the encapsulation with the thinnest possible thicknesses of the acrylic glass and the stainless steel is shown in Figure 17, its factor of safety in Figure 18.

The thickness of the hemispheres is 0.5mm for the stainless steel part and 5mm for the acrylic glass. For this PMT also the spherical encapsulation does not have an advantage compared to the conical design, but less metal is needed. The weight of the established ideal encapsulation is 5.55kg. The materials volume is 1,753.76cm<sup>3</sup> and the surface of the encapsulation comes to 10,096.48cm<sup>2</sup>, like Table 5 shows.

Spherical encapsulation:	Thickness metallic part:		0.5mm
	Thickness acrylic part:		5mm
	Volume [cm <sup>3</sup> ]	Surface [cm <sup>2</sup> ]	Weight [g]
Overall encapsulation:	1,753.76	10,096.48	5,552.94
Metallic part:	522.49	5,208.95	4,075.41
Acrylic part:	1,231.27	4,887.53	4,477.52

Table 5: Properties of the most lightweight stable spherical encapsulation for the Hamamatsu R7081 PMT in detail.

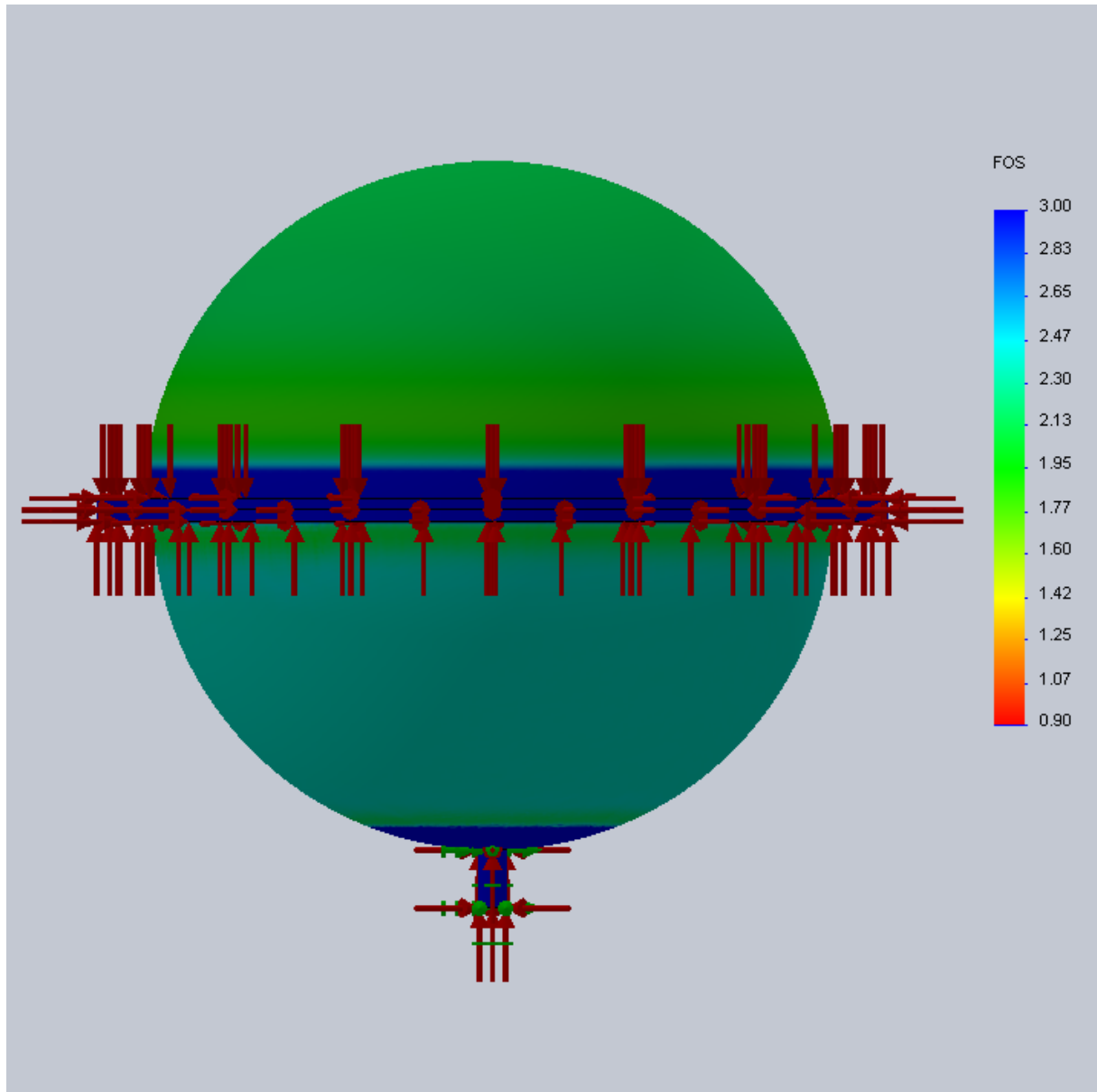


Figure 18: The factor of safety for the spherical encapsulation of the R7081 PMT. The lowest value is 1, thus the whole PMT encapsulation withstands the requested 12 bar static pressure.

### 3.5 Encapsulations for the Hamamatsu R6594 PMT

The favored 3" photomultiplier tube is the Hamamatsu R6594 PMT. In Figure 19 you can see the schematics to this photomultiplier tube. Noticeable is the small, long form of the photomultiplier tube. The measurements are 265mm in height and 128mm in width [10].

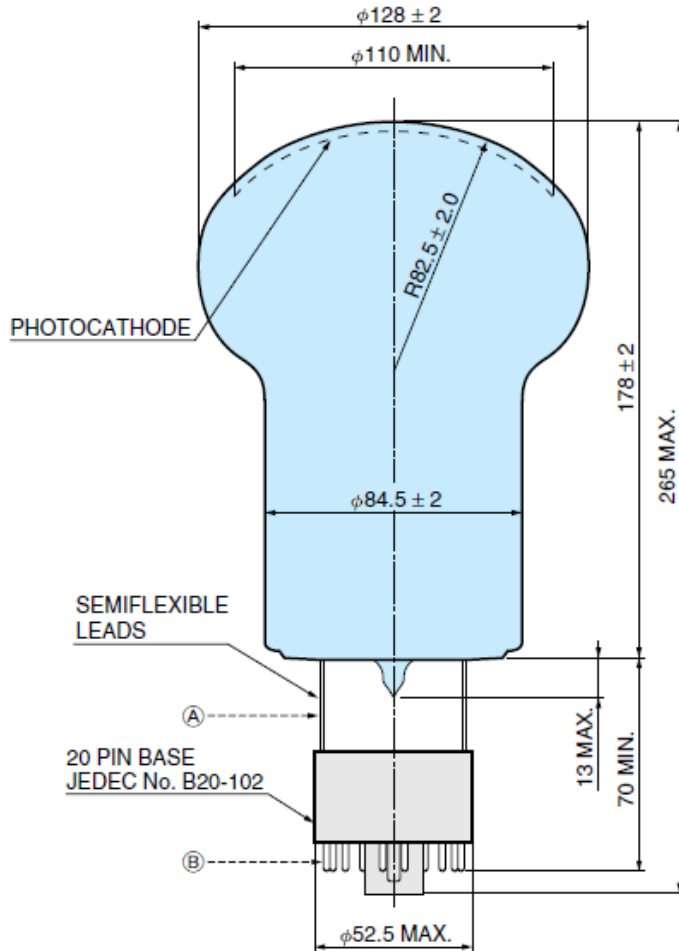
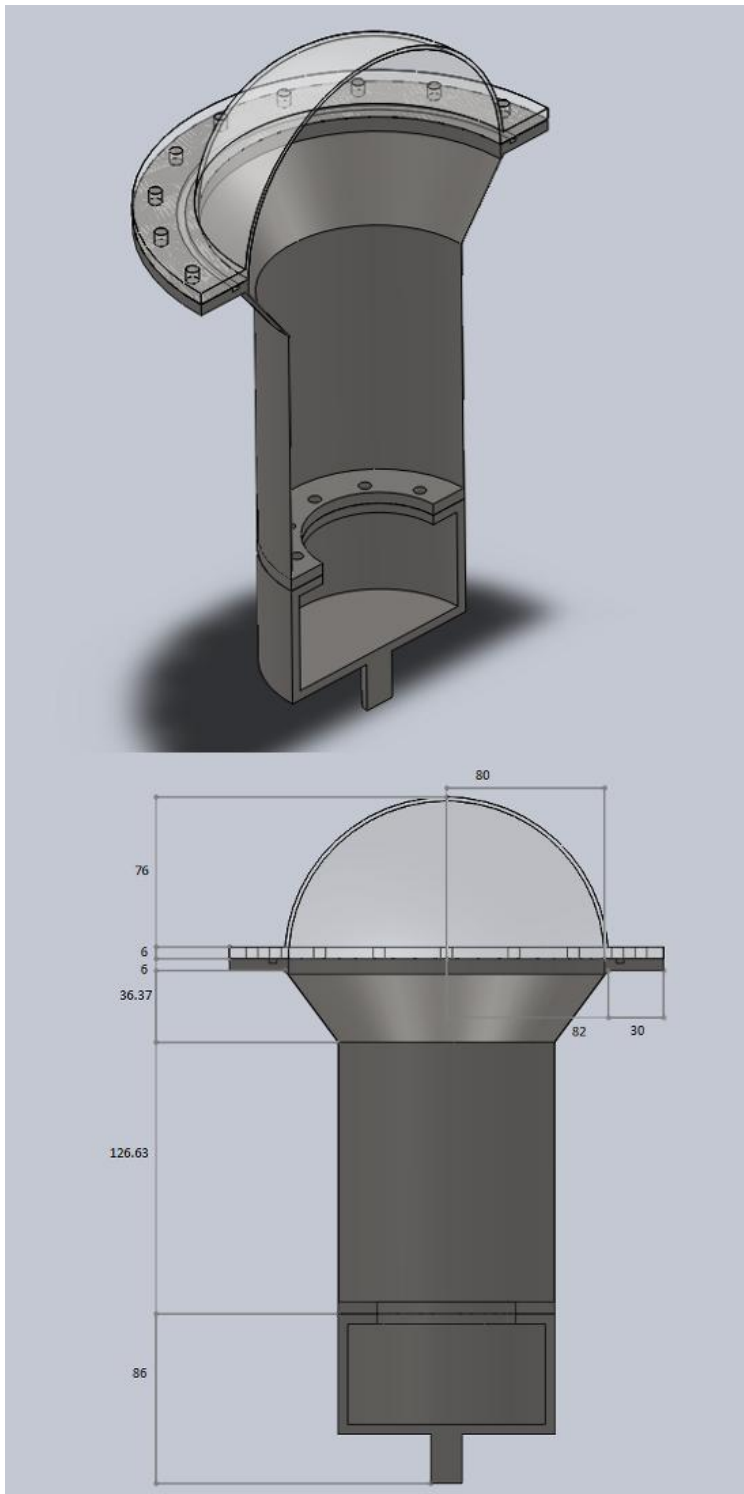


Figure 19: Profile of the Hamamatsu R6594 PMT [10]

The specific properties for this photomultiplier tube are also given in the Hamamatsu catalog. The spectral response range is from 300nm to 650nm. The quantum efficiency for this photomultiplier at the peak wavelength is also 25%. The anode dark current output, again measured after 30 minutes in complete darkness is 30nA. The transit time spread is 1.5ns at FWHM.

### 3.5.1 Conical encapsulation



For this photomultiplier tube the upper radius of the conical encapsulation is 82mm. The radius of the cylindrical part of the conic section is again 55mm. It follows for the height of the conic section a length of 36.37mm. Figure 20 shows the cross section of the conical encapsulation for the Hamamatsu R6594 PMT. The all over height of the encapsulation is 337mm.

The established minimal thicknesses of this encapsulation are 1mm for the stainless steel part and 2mm for the acrylic glass hemisphere. The factor of safety is given in Figure 21. So the complete encapsulation has a weight of 2.98kg, a materials volume of 535.77cm<sup>3</sup> and a surface of 3,678.27cm<sup>2</sup>, given in Table 6.

Figure 20: The conical encapsulation for the Hamamatsu R6594 PMT, which passed the stress test with the lowest thicknesses of 1mm for the metallic part and 2mm for the acrylic glass. The measurements are given in mm.

Conical encapsulation:	Thickness metallic part:		1mm
	Thickness acrylic part:		2mm
	Volume [cm <sup>3</sup> ]	Surface [cm <sup>2</sup> ]	Weight [g]
Overall encapsulation:	535.77	3,678.27	2,984.67
Metallic part:	354.81	2,486.83	2,767.52
Acrylic part:	180.96	1,194.43	217.15

Table 6: Properties of the most lightweight stable conical encapsulation for the Hamamatsu R6594 PMT in detail.

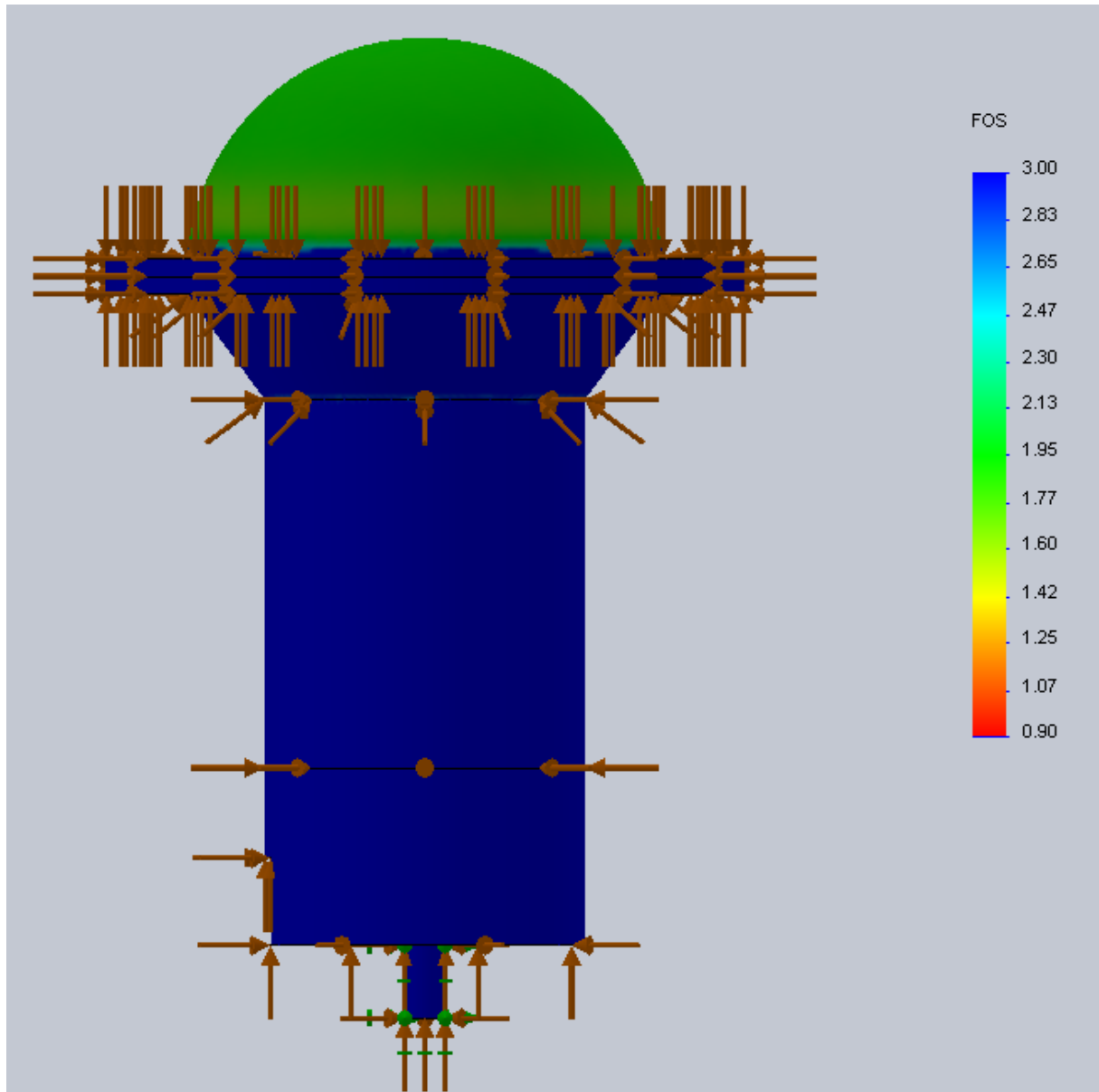
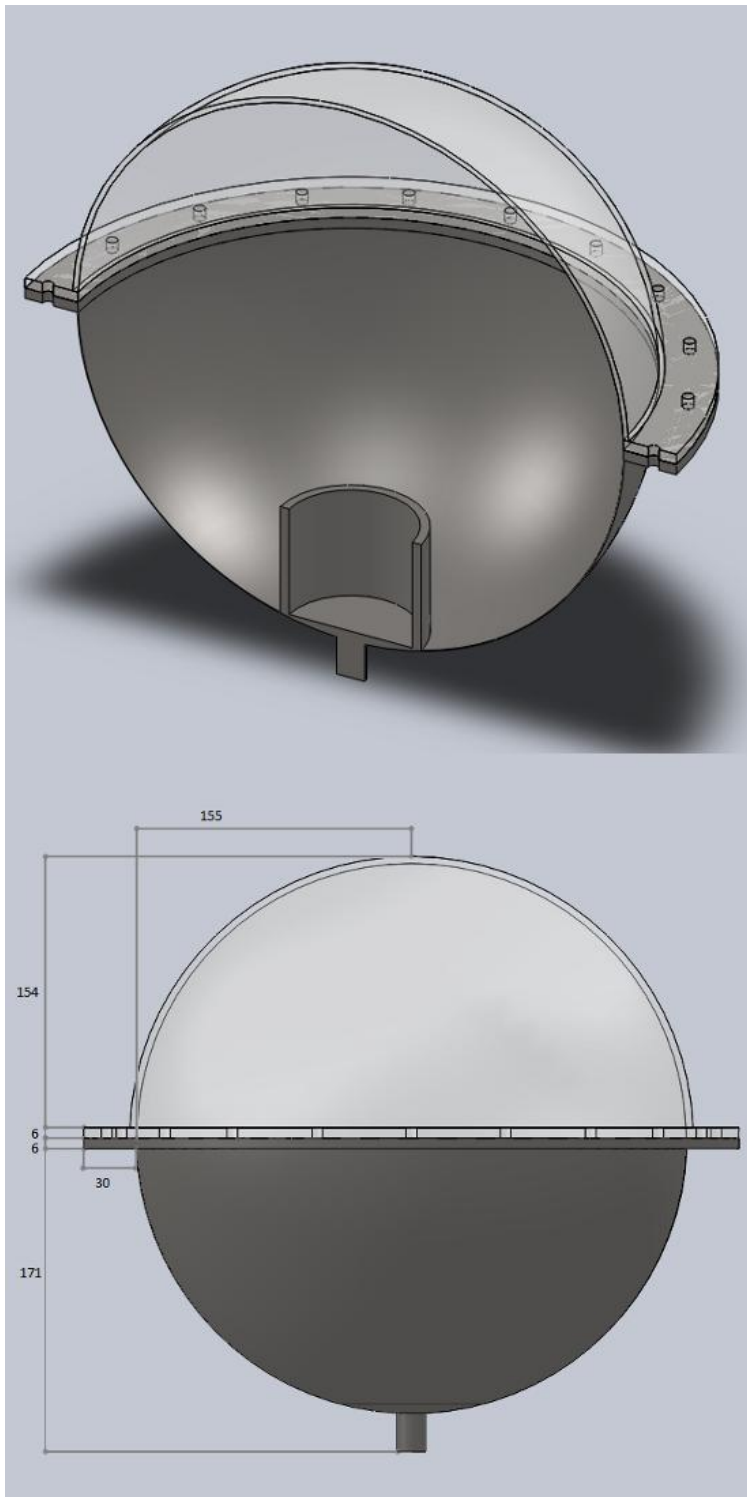


Figure 21: The factor of safety for the conical encapsulation of the R6594 PMT. The lowest value is 1.32, thus the whole PMT encapsulation withstands the requested 12 bar static pressure.

### 3.5.2 Spherical encapsulation



The spherical encapsulation for this photomultiplier tube is due to its shape unfavorable. Reason for this is the thin but relatively long form of the photomultiplier tube, which forced to build the acrylic glass and stainless steel hemispheres with a radius of 155mm, which is compared to the biggest radius of about 64mm of the photomultiplier tube very large. Figure 22 shows the cross section view of the ideal spherical encapsulation for the R6594 PMT.

The thinnest possible wall thicknesses for the R6594 PMTs spherical encapsulation, is 0.5mm for the stainless steel and 4mm for the acrylic glass. This ideal, spherical encapsulation has a weight of 3.69kg, a materials volume of 1,137.50cm<sup>3</sup> and a total surface of 7,800.93cm<sup>2</sup>. With these values, shown in table 7, the spherical encapsulation came up to the expectations, being an adverse form for the R6594 photomultiplier tube. The factor of safety is given in Figure 23.

*Figure 22: The spherical encapsulation for the Hamamatsu R6594 PMT, which passed the stress test with the lowest thicknesses of 0.5mm for the metallic part and 4mm for the acrylic glass. The measurements are given in mm.*

Spherical encapsulation:	Thickness metallic part:		0.5mm
	Thickness acrylic part:		4mm
	Volume [cm <sup>3</sup> ]	Surface [cm <sup>2</sup> ]	Weight [g]
Overall encapsulation:	1,137.50	7,800.93	3,691.83
Metallic part:	352.55	4,000.36	2,749.89
Acrylic part:	784.85	3,800.57	941.94

Table 7: Properties of most lightweight stable spherical encapsulation for the Hamamatsu R6594 PMT in detail.

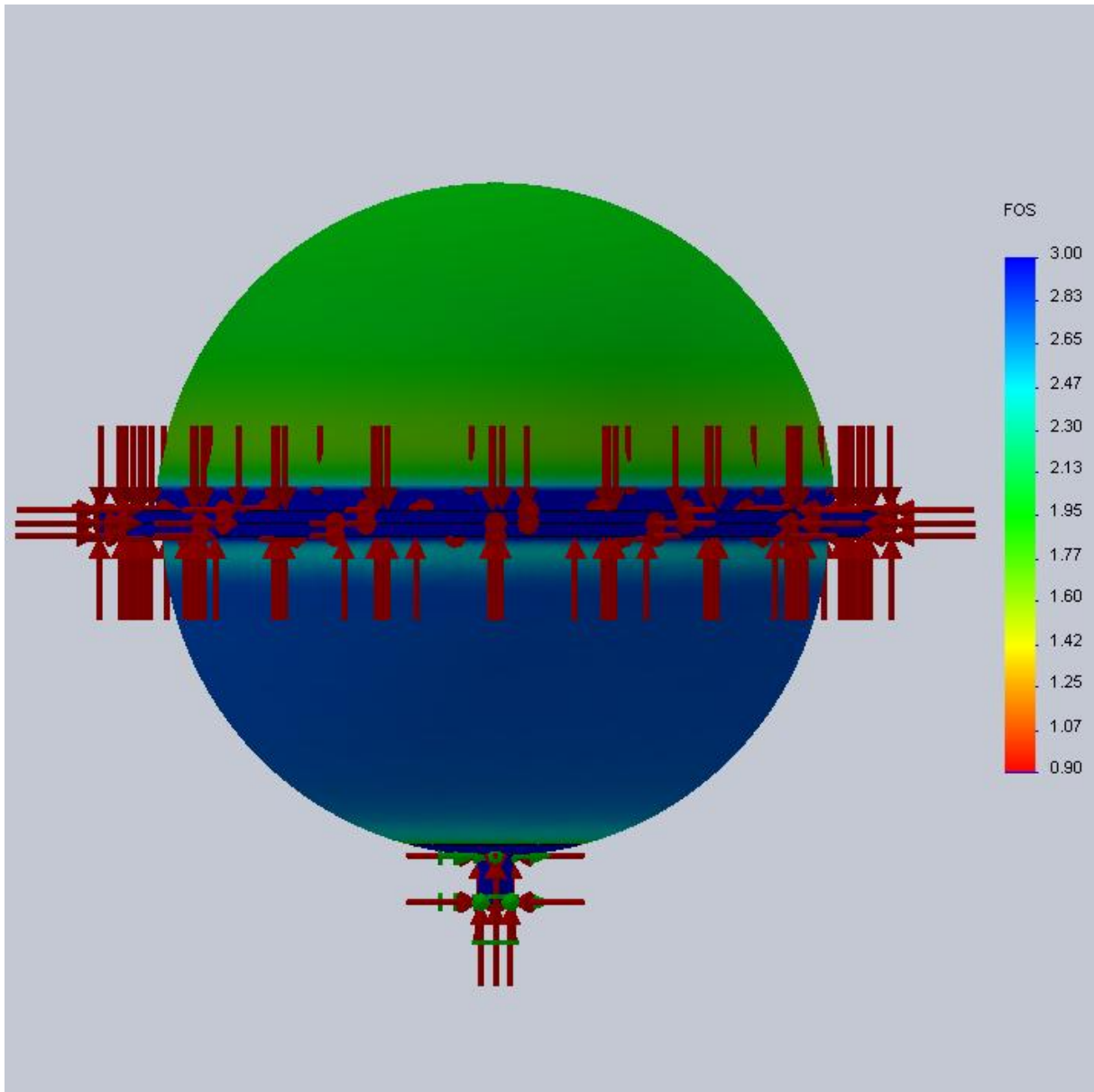
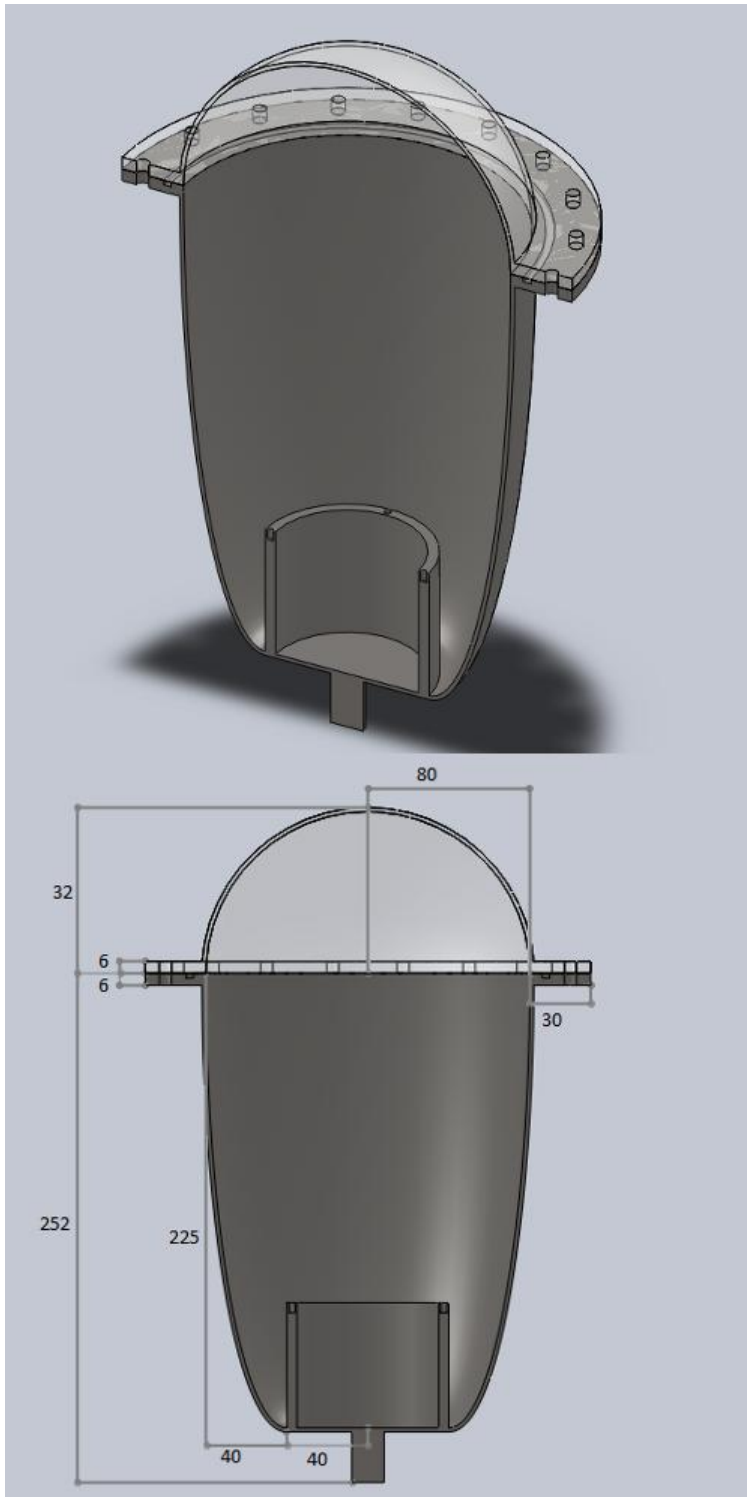


Figure 23: The factor of safety for the spherical encapsulation of the R6594 PMT. The lowest value is 1.04, thus the whole PMT encapsulation withstands the requested 12 bar static pressure.

### 3.5.3 Elliptical encapsulation



With respect to the unfavorable spherical encapsulation, an elliptical encapsulation shape with was investigated. The minor radius of the ellipse, adapted to the width of the photomultiplier tube, is 40mm. The height of the metallic encapsulation part, the major radius of the ellipse is 225mm. Figure 24 shows the assessed stable elliptical encapsulation with the least thicknesses and the corresponding factor of safety.

The necessary wall thicknesses for the elliptical encapsulation for the R6594 PMT are 2mm for the stainless steel part and even 2mm for the acrylic glass. Therewith the encapsulation has a weight of 3.28kg, a materials volume of 573.37cm<sup>3</sup> and a total surface of 4,113.30cm<sup>2</sup>, shown in Table 8.

Figure 24: The elliptical encapsulation for the Hamamatsu R6594 PMT, which passed the stress test with the lowest thicknesses of 2mm for the metallic part and 2mm for the acrylic glass. The measurements are given in mm.

Elliptical encapsulation:	Thickness metallic part:		2mm
	Thickness acrylic part:		2mm
	Volume [cm <sup>3</sup> ]	Surface [cm <sup>2</sup> ]	Weight [g]
Overall encapsulation:	573.37	4,113.30	3,277.93
Metallic part:	392.41	2,918.87	3,060.78
Acrylic part:	180.96	1,194.43	217.15

Table 8: Properties of the most lightweight stable elliptical encapsulation for the Hamamatsu R6594 PMT in detail.

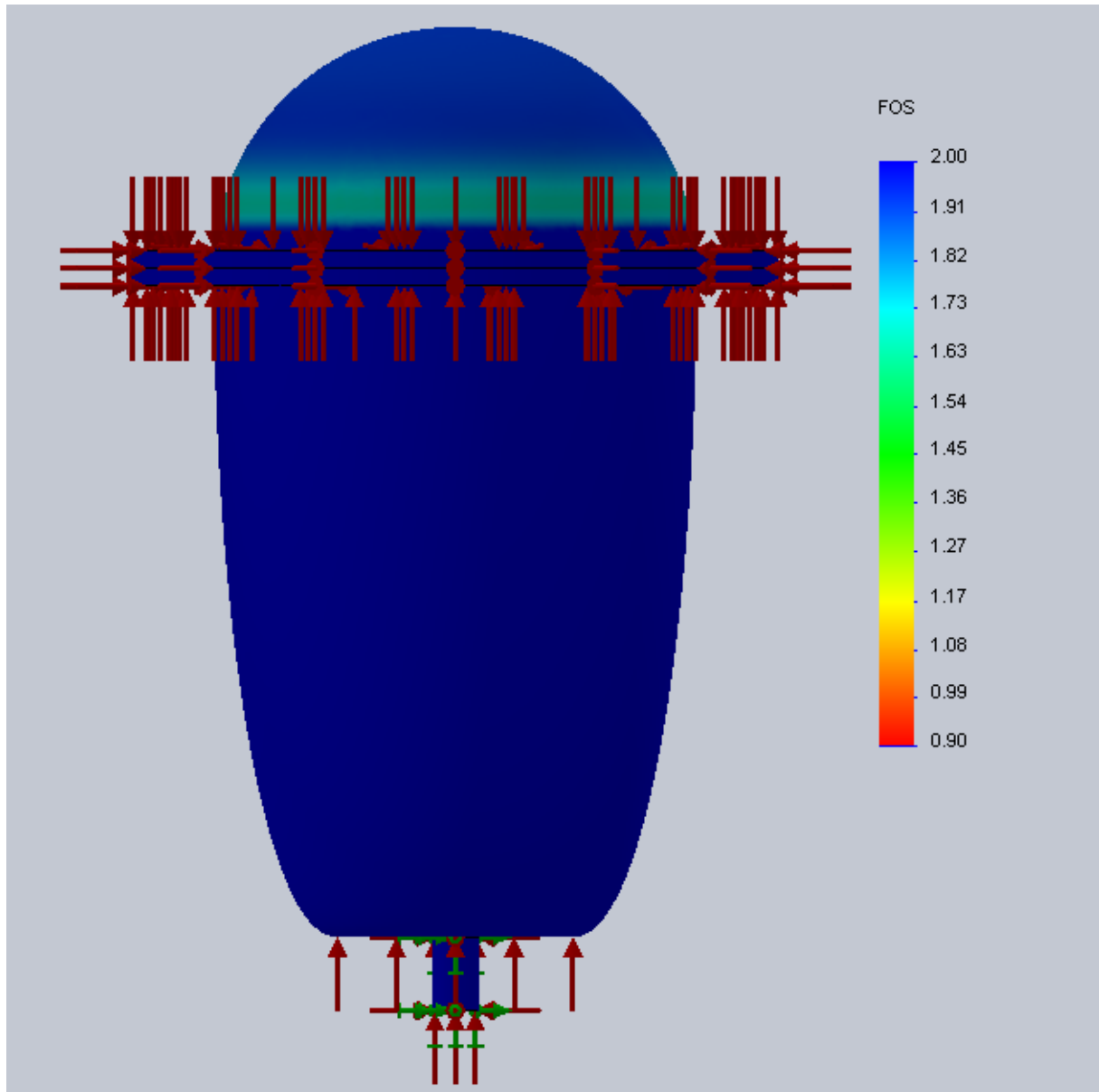
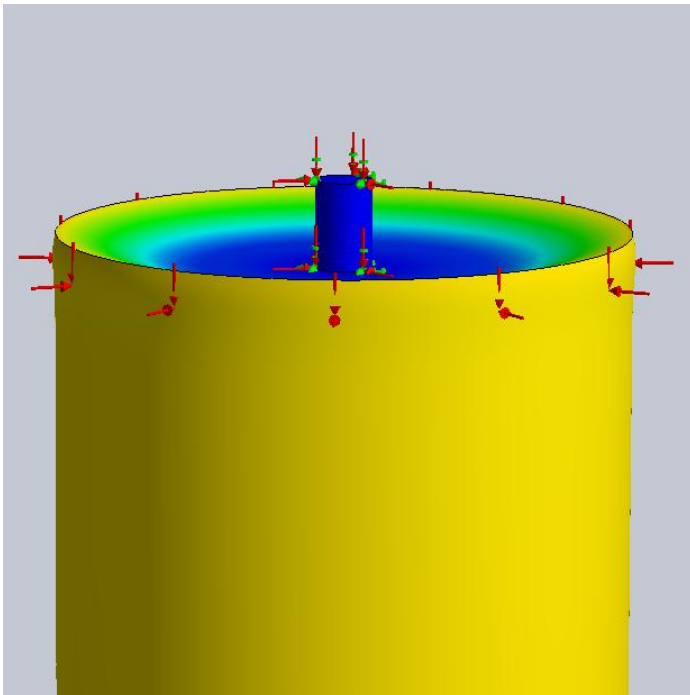


Figure 25: The factor of safety for the elliptical encapsulation of the R6594 PMT. The lowest value is 1.24, thus the whole PMT encapsulation withstands the requested 12 bar static pressure.

### 3.5.4 Cylindrical encapsulation

The first design of the cylindrical encapsulation featured the same thicknesses for the bottom and the walls of the cylinder. However, simulations show that with a thickness of 3mm the encapsulation could not withstand the pressure. The weak point of the design is the bottom, which was pressed into the encapsulation by applying pressure, shown in Figure 26. Therefore, the bottom as well as the sides of the cylinder broke because of shear strain.



*Figure 26: The first model of the cylindrical encapsulation, with a wall and bottom thickness of 3mm. By applying pressure the bottom was pressed into the encapsulation, causing structural failure.*

To solve this problem the model of the cylinder was edited by raising the thickness of the bottom of the modeled cylinders to 5mm.

The measurements of the allover cylindrical encapsulation are 337mm in height, where the metallic part alone has a height of 249mm and the radius of the encapsulation is 80mm. Figure 27 shows the established ideal cylindrical encapsulation with the least wall thicknesses, Figure 28 the factor of safety.

These thicknesses are 0.5mm for the stainless steel cylinder and 2mm for the acrylic glass hemisphere. The resulting weight is 2.83kg, the materials volume is 515.34cm<sup>3</sup> and the total surface is 4,602.41cm<sup>2</sup>, like Table 9 shows.

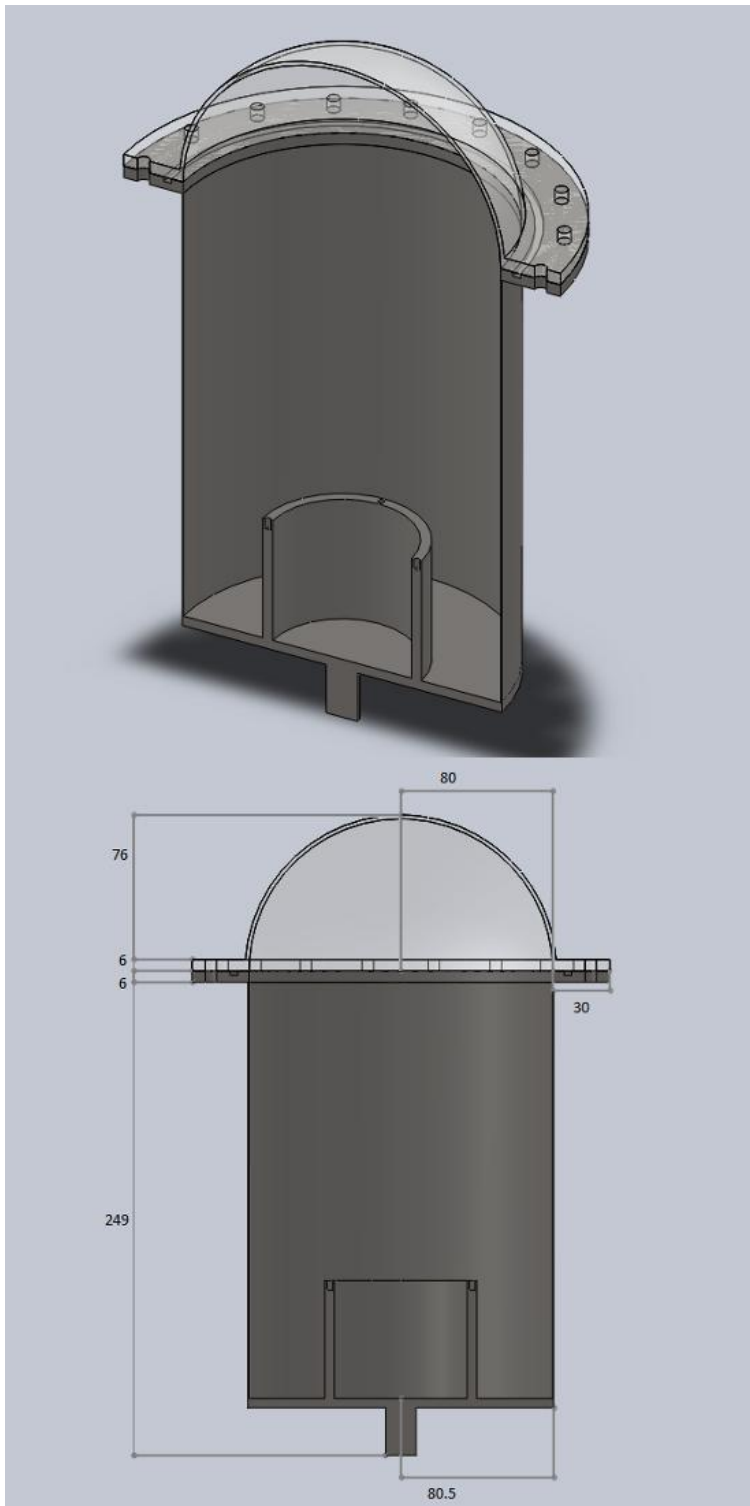


*Figure 27: The cylindrical encapsulation for the Hamamatsu R6594 PMT, which passed the stress test with the lowest thicknesses of 0.5mm for the metallic part and 2mm for the acrylic glass. The measurements are given in mm.*

Cylindrical encapsulation:	Thickness metallic part:		0.5mm
	Thickness acrylic part:		2mm
	Volume [cm <sup>3</sup> ]	Surface [cm <sup>2</sup> ]	Weight [g]
Overall encapsulation:	515.34	4,602.41	2,825.30
Metallic part:	334.38	3,407.98	2,608.15
Acrylic part:	180.96	1,194.43	217.15

Table 9: Properties of the most lightweight stable cylindrical encapsulation for the Hamamatsu R6594 PMT in detail.

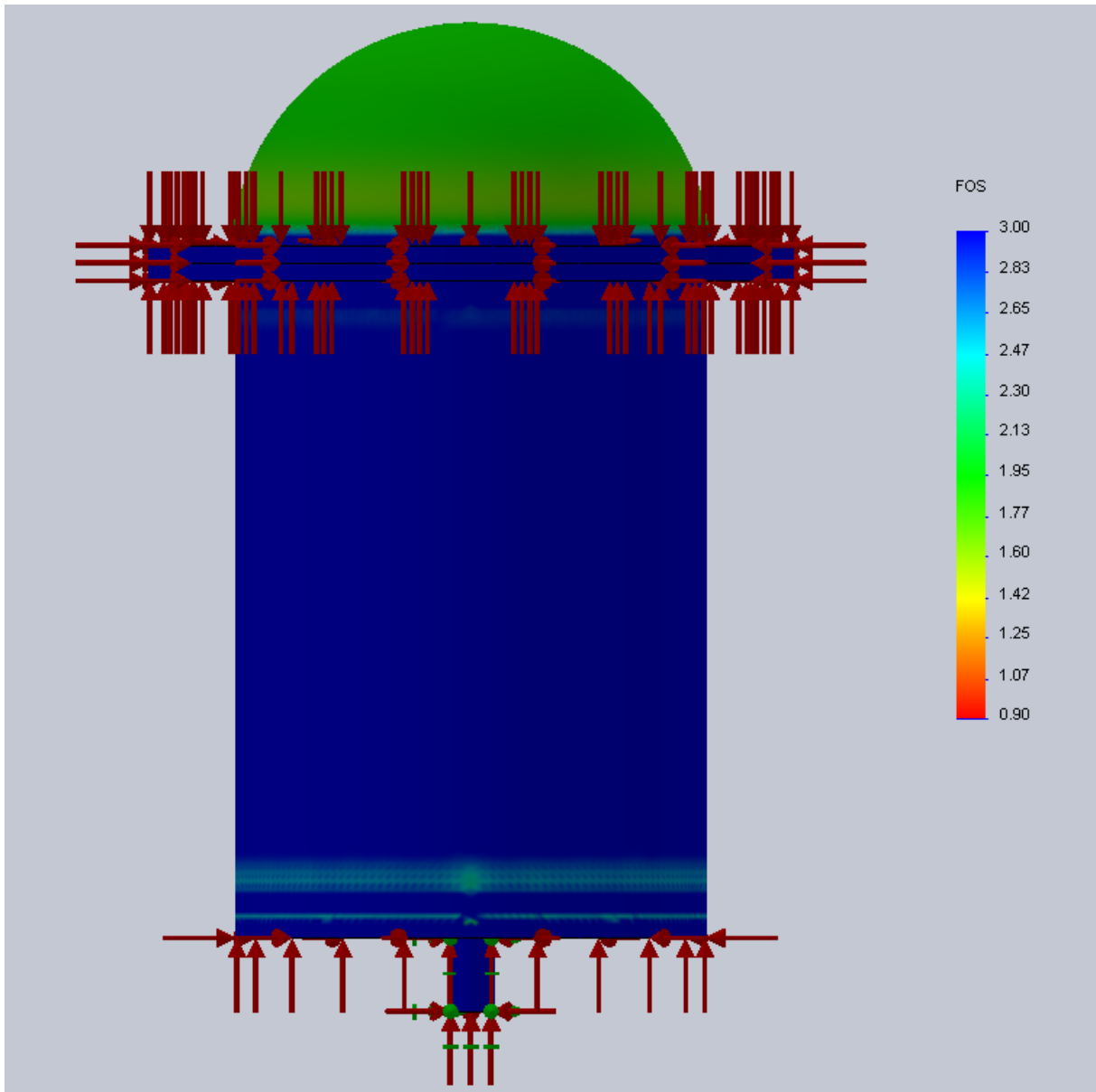


Figure 28: The factor of safety for the cylindrical encapsulation of the R6594 PMT. The lowest value is 1.21, thus the whole PMT encapsulation withstands the requested 12 bar static pressure.

## 4. PMT arrangement in the inner detector

The installing of the photomultiplier tubes on the inner surface of the detectors walls was also briefly investigated in this bachelor thesis. Thereby a hexagonal arrangement of the photomultiplier was studied. First of all, the distances of the photomultiplier tubes had to be calculated. For that reason the entrance aperture radius of the Winston cones was computed. This aperture radius depends on the photosensitive area of the particular photomultiplier tube and the area increase factor  $m$  of the Winston cone. An area increase factor of 1.75 was used in the calculation. The radii  $r_{p.a.}$  of these surfaces are even given in Figure 9, Figure 14 and Figure 19 for each PMT. The entrance aperture radius  $r_{e.a.}$  was calculated by the formula:

$$r_{e.a.} = \sqrt{1.75} \cdot r_{p.a.} \quad (2)$$

Table 10 shows these results.

Finally, an optical coverage of 30% is targeted, so the entrance aperture area of the PMTs within a hexagon has to be 30% of the hexagons area. Figure 29 shows that one PMT is completely within this area of a hexagon and each of the six PMTs at the edges of the hexagon cover the hexagons surface with one third of the entrance aperture area.

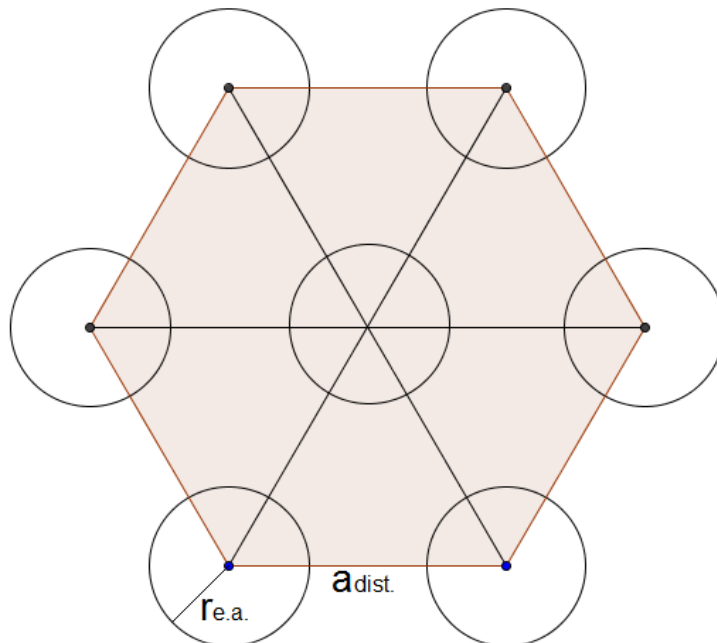


Figure 29: Schematic hexagon with a 30% area coverage.

Therefore formula (3) is arising thereby:

$$3 \cdot A_{e.a.} = 0.3 \cdot A_{Hexagon}$$

$$3 \cdot \pi \cdot r_{e.a.}^2 = 0.3 \cdot \frac{3}{2} \cdot a_{dist.}^2 \cdot \sqrt{3} \quad (3)$$

Here is  $a_{dist.}$  the edge length of the hexagon and the distance of two neighboring PMTs.

Table 10 shows the distances and the radii of the entrance aperture for each type of PMT.

PMT	$r_{p.a.}$ [mm]	$r_{e.a.}$ [mm]	$a_{dist.}$ [mm]
R5912	95	125.67	473.01
R7081	110	145.52	506.01
R6594	55	72.76	253.00

*Table 10: The radii of the photosensitive area, the entrance aperture and the calculated distances between the photomultiplier tubes necessary for an optical coverage of 30%.*

Here occurs a problem with the spherical encapsulation for the R6594 PMT. Due to the encapsulations width of 370mm no optical coverage of 30% could be reached.

However, a possible array of cylindrical encapsulations of the R6594 PMT is shown as an example in Figure 30. Thereby the calculated distance, for increased photosensitive area with Winston cones, was used, but these are not shown in the figure. The bracket is fixed on the small cylinders on the bottom of the encapsulations as well as on the flange.

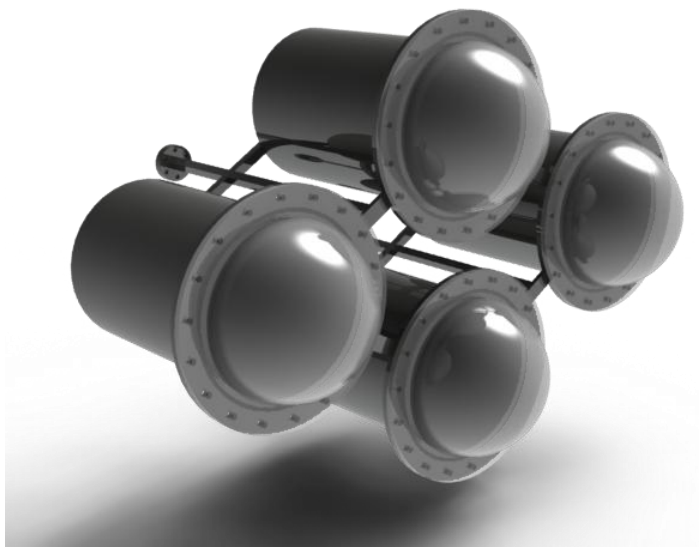


*Figure 30: A segment of 4 PMT encapsulations. The distance is adjusted to an optical coverage of 30%, using Winston cones*

## 5. Summary and outlook

In this thesis, a variety of encapsulation models for 3 photomultiplier tubes of Hamamatsu (R5912, R7081 and R6594) were designed and their pressure resistance systematically studied with a Finite Element Method within the framework of the CAD program SolidWorks.

Based on this analysis, it can be concluded that conical encapsulations are the favorable design for the studied photomultiplier tubes. The conical encapsulations have fewer surfaces compared to the other designs, and thus a more suitable for an ultra-low radioactivity experiment like LENA. Only the cylindrical encapsulation for the R6594 PMT might be an option due to less material is needed.

Table 11 at the end of this chapter summarizes the properties of the studied encapsulations.

As demonstrated in this thesis, SolidWorks is a very powerful tool for the design of PMT encapsulations for LENA.

There are other simulations, which could be done with this software. SolidWorks is able to calculate the deformation of the encapsulation parts. Figure 31 shows one of these simulations as an example, done for a spherical encapsulation for the R6594 PMT. The encapsulation shows such a significant deformation of the acrylic glass (with a thickness of 2mm), that the acrylic glass will break. If a stable encapsulation is deforming this much without breaking and the PMT gets touched by glass, there is the danger of damaging the PMT. In this case, the encapsulation's thickness or shape would have to be modified.

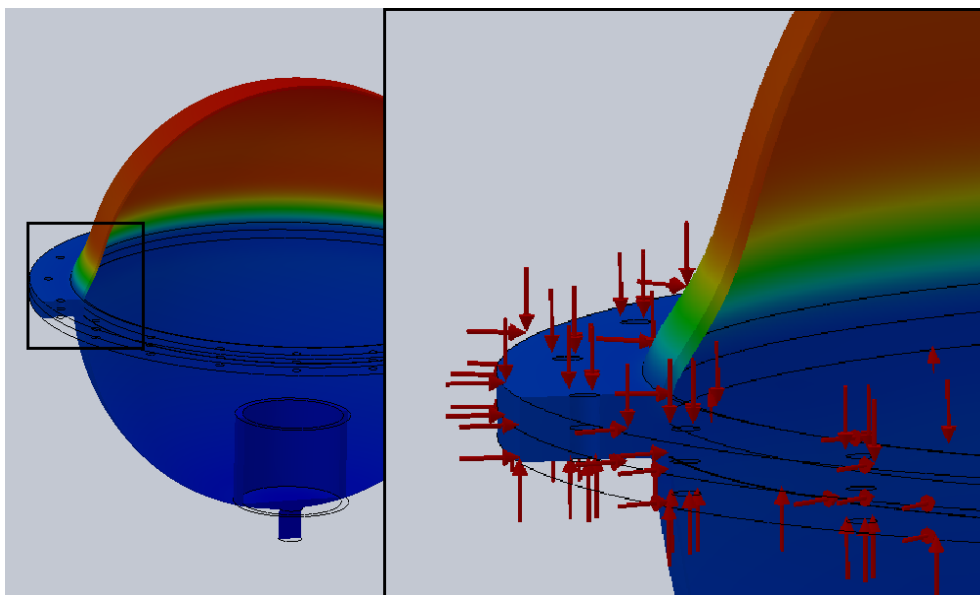


*Figure 31: The deforming spherical encapsulation with wall thicknesses of 0.5mm stainless steel and 2mm acrylic glass, done for the Hamamatsu R6594 photomultiplier tube. Please note: The acrylic glass of 2mm thickness does not stand the pressure of 12 bar.*

Furthermore the meshing could be improved by reducing the node distances. Depending on the processing power of the simulating computer, this could be done for the whole model or only at the critical edges.

Also the inside of the encapsulations has to be considered. So ideas have to be found how the base and the PMT in the encapsulation could be fixed so they cannot come loose.

Moreover the encapsulations have to contain Mu-metal. The attachment of the Mu-metal into the encapsulations, as well as the mounting of Winston-cones are still open tasks in the design process of LENA.

Finally the study could be extended to additional photomultiplier tubes, which could be used for the LENA project. Candidates for such a study would be the Hamamatsu PMT called R6091, which is a 3" photomultiplier tube and photomultiplier tubes of the Electron Tubes Enterprises Ltd..

<b>PMT R5912</b>			
<b>Conical encapsulation:</b>	<b>Thickness metallic part:</b>		<b>1mm</b>
	<b>Thickness acrylic part:</b>		<b>3mm</b>
	Volume [cm <sup>3</sup> ]	Surface [cm <sup>2</sup> ]	Weight [g]
Properties:	829.25	5,315.85	3,733.22
<b>Spherical encapsulation:</b>	<b>Thickness metallic part:</b>		<b>0.5mm</b>
	<b>Thickness acrylic part:</b>		<b>4mm</b>
	Volume [cm <sup>3</sup> ]	Surface [cm <sup>2</sup> ]	Weight [g]
Properties:	1,509.86	8,346.03	5,752.82
<b>PMT R7081</b>			
<b>Conical encapsulation:</b>	<b>Thickness metallic part:</b>		<b>2mm</b>
	<b>Thickness acrylic part:</b>		<b>4mm</b>
	Volume [cm <sup>3</sup> ]	Surface [cm <sup>2</sup> ]	Weight [g]
Properties:	1,277.15	6,921.98	5,236.68
<b>Spherical encapsulation:</b>	<b>Thickness metallic part:</b>		<b>0.5mm</b>
	<b>Thickness acrylic part:</b>		<b>5mm</b>
	Volume [cm <sup>3</sup> ]	Surface [cm <sup>2</sup> ]	Weight [g]
Properties:	1,753.76	10,096.48	5,552.94
<b>PMT R6594</b>			
<b>Conical encapsulation:</b>	<b>Thickness metallic part:</b>		<b>1mm</b>
	<b>Thickness acrylic part:</b>		<b>2mm</b>
	Volume [cm <sup>3</sup> ]	Surface [cm <sup>2</sup> ]	Weight [g]
Properties:	535.77	3,678.27	2,984.67
<b>Spherical encapsulation:</b>	<b>Thickness metallic part:</b>		<b>0.5mm</b>
	<b>Thickness acrylic part:</b>		<b>4mm</b>
	Volume [cm <sup>3</sup> ]	Surface [cm <sup>2</sup> ]	Weight [g]
Properties:	1,137.50	7,800.93	3,691.83
<b>Elliptical encapsulation:</b>	<b>Thickness metallic part:</b>		<b>2mm</b>
	<b>Thickness acrylic part:</b>		<b>2mm</b>
	Volume [cm <sup>3</sup> ]	Surface [cm <sup>2</sup> ]	Weight [g]
Properties:	573.37	4,113.30	3,277.93
<b>Cylindrical encapsulation:</b>	<b>Thickness metallic part:</b>		<b>0.5mm</b>
	<b>Thickness acrylic part:</b>		<b>2mm</b>
	Volume [cm <sup>3</sup> ]	Surface [cm <sup>2</sup> ]	Weight [g]
Properties:	515.34	4,602.41	2,825.30

Table 11: The properties of the assessed ideal encapsulations with the lowest but stable thicknesses.

## Bibliography:

- [1] Soapbox Science: [http://blogs.nature.com/soapbox\\_science/2011/03/02/ghosts-of-the-universe](http://blogs.nature.com/soapbox_science/2011/03/02/ghosts-of-the-universe), (24.07.2011)
- [2] Peter Fierlinger: “Kern-Teilchen-Astrophysik” lecture, TUM, WS 2010/2011
- [3] Michael Wurm: “Cosmic Background Discrimination for the Rare Neutrino Event Search in BOREXINO and LENA.” PhD thesis, TUM.
- [4] Homepage of the Research Group Neutrino Physics of the University Hamburg: <http://neutrino.desy.de/projekte/lena>, (30.07.2011)
- [5] M.Wurm et al.: “The next-generation liquid-scintillator neutrino observatory LENA”, Whitepaper for LENA, 1104.5620v2 (2011)
- [6] Marc Tippmann: Talk “Detector development”, ANT2010 Santa Fe, (18.09.2011)
- [7] Hamamatsu photonics K.K. Editorial Committee: “Photomultiplier tubes – Basics and Applications”, Third edition, February 2006
- [8] Super-Kamiokande Homepage: <http://www-sk.icrr.u-tokyo.ac.jp/sk/gallery/index-e.html>, (09.07.2011)
- [9] SolidWorks Help: <http://help.solidworks.com/2011/German/SolidWorks/sldworks/LegacyHelp/Sldworks/Overview/StartPage.htm>, (31.07.2011)
- [10] Hamamatsu photonics K.K.: Catalog: “Photomultiplier tubes and assemblies”, June 2009

## Danksagung:

An erster Stelle möchte ich Herrn Prof. Lothar Oberauer für die Themenstellung danken, da ich dadurch Einblick in ein sehr interessantes Projekt erhalten habe. Desweiteren erlaubte mir diese Arbeit einen Einblick in SolidWorks, womit ich mich sehr gerne beschäftigt habe. Die Betreuung durch Herrn Oberauer war sehr gut und er schaffte von Beginn an eine sympathische Arbeitsatmosphäre, die mir die Angst vor dem Neuland Bachelorthesis recht schnell nahm. Vielen Dank dafür.

Marc Tippmann möchte ich für seine hervorragende Unterstützung bei der Einweisung ins Projekt, sowie bei der Arbeit an sich danken. Für seine Bachelorstudenten hatte er sich immer Zeit genommen, auch wenn er eigentlich keine hatte. Damit schaffte er es, mir durch die Sicherheit jederzeit einen direkten Ansprechpartner zu haben, ein angenehmes Arbeiten zu ermöglichen.

Weiterer besonderer Dank geht an Herrn Harald Hess, Werkstattleiter des Lehrstuhls, der mir bei allen technischen Fragen, sowie bei allen Fragen zu SolidWorks immer höchst kompetent zur Verfügung stand. Er hat mir das Einarbeiten in die Software sehr erleichtert.

Die gesamte Kollegschaft des Lehrstuhls war sehr freundlich und hilfsbereit und hat eine sehr angenehme, lockere Arbeitsatmosphäre geschaffen, an der ich gerne teilgenommen habe. Besonders hervorheben möchte ich dabei nochmals Marc Tippmann, sowie Quirin Meindl, Jürgen Winter und Timo Lewke, die bei Fragen immer zur Stelle waren und durch ihre sympathische Art sehr angenehme Kollegen waren.

Herzlicher Dank geht auch an meine Familie, sowie besonders an meine Freundin. Sie haben es geschafft in Zeiten großen Stresses mir Halt und Ruhe zu geben. Vielen Dank.